# Introduction of many-body physics of fermions and bosons

Master 2 ICFP

Pascal Simon and Michele Casula

25 février 2021

# Table des matières

# Chapitre 1

# Introduction

Ideally, we would like to solve the Schrödinger equations

$$\left[-\frac{\hbar^2}{2m}\sum_{j=1}^{N}\nabla_j^2+\sum_{i<j}V(|\mathbf{r}_i-\mathbf{r}_j|)+\sum_j U(\mathbf{r}_i)\right]\Psi=i\hbar\frac{\partial\Psi}{\partial t}, \tag{1.1}$$

where $\Phi \equiv= \Psi(\mathbf{r}_1,\cdots,\mathbf{r}_N)$. This would allow us to determine both the eigenfunctions and eigenspectrum of the many-body Hamiltonian. Why trying to solve such problem ? Beyond the academic problem, we may have in mind to deal charge fermions interacting with a Coulomb potential $V(r)=q^2/(4\pi\epsilon_0 r)$ where $q$ denotes the charge. Therefore solving the above Schrödinger equation would allow us to describe accurately interacting electrons in a solid or in a condensed matter phase. We may have also in mind to describe the problem of Rydberg atoms in a trap potential. The 2-body interacting would then be a long-range dipolar interaction $V(r)\sim 1/r^3$).

If we have an electromagnetic field, we need to substitute

$$\nabla \longrightarrow \nabla - iq\mathbf{A} \tag{1.2}$$

$$U(\mathbf{r}) \longrightarrow U(\mathbf{r}) + q\Phi(\mathbf{r}), \tag{1.3}$$

where $\mathbf{A}$ is the gauge vector and $\Phi$ the electric potential.

Obviously, in a typical condensed matter system, with $N\sim 10^{23}$, the Hilbert space grows exponentially too fast to hope to solve such Schrödinger equation.

In a cold atomic system which has only a few atoms trapped in a low-dimensional potential, diagonalizing directly the Hamiltonian may actually be a good way to approach this problem. At least, this may allow to calibrate the experiment in some range of parameters. Beyond what is presently achievable numerically, cold atoms trapped in an optical potential can then offer an interesting platform for in situ quantum simulations.

However, we learnt fom statistical physics, that we do not need to solve the equation of motion of $N$ bodies to be able to predict some macroscopic **emergent** behaviour. Can we expect a similar strategy to hold here ?

Although the notion of emergence is certainly playing a major role in modern quantum many-body physics, for a general many-body problem this is difficult to predict based only on symmetries and dimensionality what kind of low-energy physics is about to emerge. This is typically problem-dependent. This is why many numerical tools have been fastly developing over the past decades to tackle these kinds of problems.

The strategy developed in this lecture is rather pedestrian. We need a known starting point. We will therefore start with the non-interacting problem and swich on the interactions. We will then learn how to treat the interaction perturbatively in order to compute some observables. This will allows us to indroduce the Green function formalism. The second part of the lecture will be devoted to some modern numerical approach to many-body phsyics.

## 1.1 Kinetic energy (band structure)

### 1.1.1 Band structure

Let us consider free particles in a box with periodic boundary conditions ($V=U=0$ above). Using translation invariance, the Hamiltonian is diagonal in the plane-wave basis and can be written in a second-quantized form as

$$H=\sum_{\mathbf{k},\sigma}\epsilon(k)c^\dagger_{\mathbf{k},\sigma}c_{\mathbf{k},\sigma}, \tag{1.4}$$

with $\epsilon(k) = \hbar^2 k^2/2m$ the dispersion relation. Here $c^\dagger_{\mathbf{k},\sigma}$ creates a particle with momentum $\mathbf{k}$ and spin $\sigma$. The symbol $\sigma$ denotes typically the spin quantum number but can also encapsulate extra quantum numbers. For $N$ fermions, the ground state $|GS\rangle$ is obtained by filling up the $N$ lowest energy states :

$$|GS\rangle \equiv c^\dagger_{k_p\uparrow} c^\dagger_{k_p\downarrow} \cdots c^\dagger_{k_1\uparrow} c^\dagger_{k_p\downarrow} |0\rangle, \tag{1.5}$$

assuming $N = 2p$ and $\epsilon(k_1) < \cdots < \epsilon(k_p)$. This approach can be obviously extended to the case where we do have many bands. Although the Hamiltonian being non-interacting, classifying all possible non-interacting hamitlonians has received a considerable interest in the past decade and our understanding of band structure has been completely revolutionized with the emergence of topology in Bloch space. However, this is another field which I will not touch (see e.g. [1]).

Before closing this paragraph, let us remind the behaviour of the density of states as a function of the dimension $d$. The density of particles is defined by $n = N/V$ where $N = \langle GS|\hat{N}|GS\rangle$.

Let us first consider $d = 3$.

$$N = \langle GS| \sum_{\mathbf{k},\sigma} n_{\mathbf{k},\sigma} |GS\rangle \approx \frac{V}{(2\pi)^3} \sum_\sigma \int_0^{k_F} dk (4\pi k^2) = \frac{V k_F^3}{3\pi^2}. \tag{1.6}$$

We thus obtain $n = \frac{k_F^3}{3\pi^2}$. For a quadratic dispersion relation $\epsilon = \frac{\hbar^2 k^2}{2m}$, we can therefore the energy dependence of the density as

$$n(\epsilon) = \frac{1}{3\pi^2} (\frac{2m}{\hbar^2})^{3/2} \epsilon^{3/2}. \tag{1.7}$$

Therefore, for a 3D metal, the density of states $\rho(\epsilon) = dn/d\epsilon$ (per unit volume) scales as $\rho(\epsilon) = \frac{1}{2\pi^2}(\frac{2m}{\hbar^2})^{3/2}\epsilon^{1/2}$. Similarly, one can calculate the ground state energy as $E^0_{3D} = \langle GS| \sum_{\mathbf{k},\sigma} \frac{\hbar^2 k^2}{2m} |GS\rangle = \frac{3}{5} N \epsilon_F$. Hence, the ground state energy per particle scales as $E^0_{3D}/N \sim n^{2/3}$. For a typical metal, $n \sim 10^{29}$ m$^{-3}$, $k_F \sim 13.6$ nm$^{-1}$ and $\lambda_F \sim 0.46$nm which implies 2-3 lattice distance.

One can repeat these calculations in $d = 2$. The density of particles reads as $n(\epsilon) = \frac{m}{\pi\hbar^2}\epsilon$ which implies a constant density of states. Similarly, one shows that the ground state energy per particle scales as $E^0_{2D}/N \sim n$.

Exercice : Perform the same analysis as above with a linear dispersion relation instead of a quadratic one.

### 1.1.2 Tight-binding model

We use above a continuum limit formulation. However in a solid, electrons are attached to an atom. We may therefore use a tight-binding formulation. A one-dimensional tight-binding hamiltonian reads

$$\hat{H} = -t \sum_j c^\dagger_j c_{j+1} + h.c.), \tag{1.8}$$

where the index $j$ corresponds to a lattice site. We omit the spin index to lighten notations. In Fourier space, we introduce $c_k$ such that

$$c_j = \frac{1}{\sqrt{N}} \sum_k c_k e^{i\mathbf{k}\cdot\mathbf{r}_j}, \tag{1.9}$$

such that

$$\hat{H} = \sum_k \varepsilon_k c^\dagger_k c_k, \tag{1.10}$$

where

$$\varepsilon_k = -2t \cos ka.$$

Let us consider the case where $\varepsilon_F = 0$. This corresponds to half-filling where $\mu = \varepsilon_F = 0$. The low-energy excitations of such a Hamiltonian are confined near the Fermi level namely for $k \simeq k_F = \pm\frac{\pi}{2a}$. Linearizing the dispersion relation, we have in the limit $(k - k_F)a \ll 1$ (see Fig. 1.1)

$$\begin{aligned} \varepsilon_k &= 2t \sin\left[(k - k_F)a\right] \\ &\simeq 2ta(k - k_F). \end{aligned}$$

Therefore, in the low-energy approximation, we have linearized the spectrum to write around $k > 0$

$$\varepsilon_k = \hbar v_F (k - k_F). \tag{1.11}$$

where $\hbar v_F = 2ta$. We obtain the same result for $k < 0$ linearizing around $-k_F$. We have thus obtained an **effective** Hamiltonian valid at low-energy, i.e. $|\varepsilon| \ll t$, which does not depend on the details occuring at high energy. Conversely, this also implies that observables mesured in this low-energy range do not depend on the high-energy details of the band structure. This is important since observables may become universal in the low-energy regime and therefore worth being studied.

Notice the emergence of some Lorentz invariance in this low-energy Hamiltonian which is not present in the initial tight-binding Hamiltonian. Indeed, quite often the symmetries may be larger at low-energy than in the initial starting Hamiltonian.

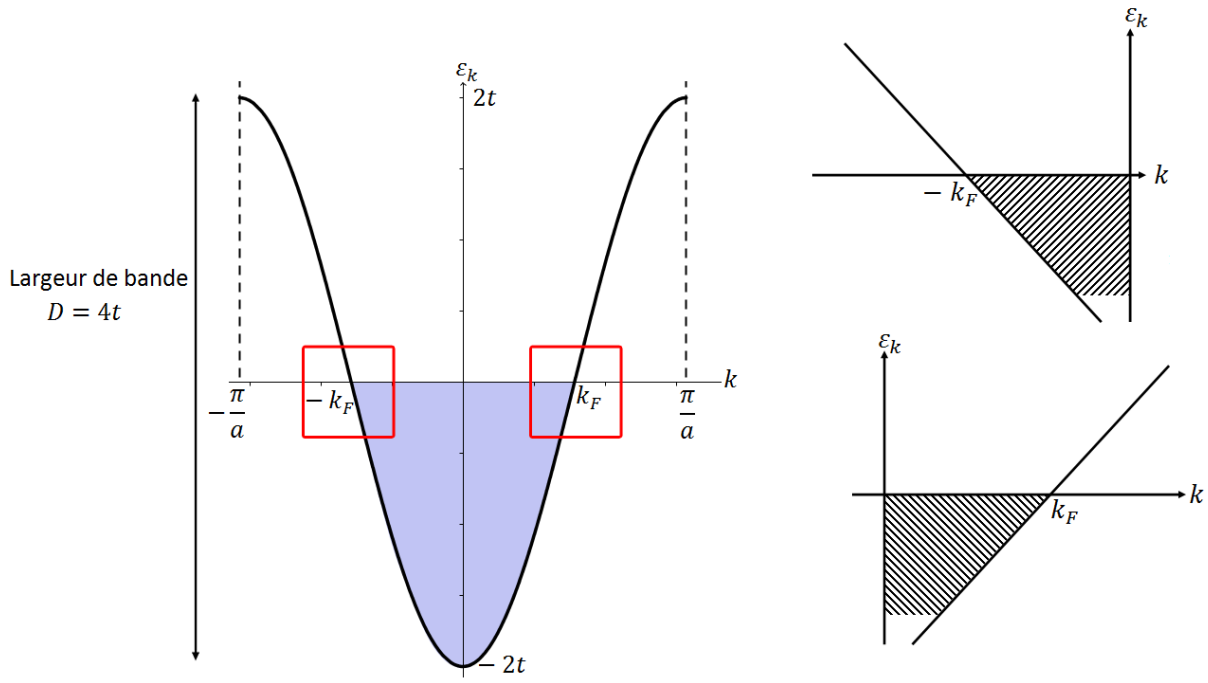


(a) (b)

FIGURE 1.1 – (a) Initial dispersion of the system with bandwidth $D = 4t$. Near the Fermi level, we can linearize this spectrum (b) a new dispersion relation valid only at low energy.

## 1.2 Interactions and Fermi liquids

Lt us now consider the Hamiltonian

$$\hat{H} = \sum_{k,\sigma} \varepsilon_k c^\dagger_{k,\sigma} c_{k,\sigma} + \frac{1}{2V} \sum_{\mathbf{q},\mathbf{k}_1,\mathbf{k}_2,\sigma_1,\sigma_2} \mathcal{V}(q) c^\dagger_{\mathbf{k}_1+\mathbf{q},\sigma_1} c^\dagger_{\mathbf{k}_2-\mathbf{q},\sigma_2} c_{\mathbf{k}_2,\sigma_2} c_{\mathbf{k}_1,\sigma_1}, \tag{1.12}$$

where the second term is the Fourier transform of the Hamiltonian

$$\frac{1}{2} \int \sum_{\sigma_1,\sigma_2} d\mathbf{r}_1 d\mathbf{r}_2 \mathcal{V}(|\mathbf{r}_1 - \mathbf{r}_2|) \hat{\psi}^\dagger_{\sigma_1}(\mathbf{r}_1) \hat{\psi}^\dagger_{\sigma_2}(\mathbf{r}_2) \hat{\psi}_{\sigma_2}(\mathbf{r}_2) \hat{\psi}_{\sigma_1}(\mathbf{r}_1).$$

Such interaction can be the Coulomb one in which case

$$\mathcal{V}_{\text{Coulomb}}(q) = \frac{e^2}{\varepsilon_0 q^2}, \ \mathcal{V}_{\text{Coulomb}}(r) = \frac{e^2}{4\pi\varepsilon_0 r}.$$

in $D = 3$. In the case of Copper, its electronic orbital structure is $3d^{10}4s^1$. This implies one conduction electron par atom. Its average density is $n_e = 8,4.10^{22} cm^{-3}$ which implies an average distance between electron $d = n_e^{-1/3} =$

$2,3$Åand therefore an average Coulomb interaction $\mathcal{V}_{\text{Coulomb}}(d) = \frac{e^2}{4\pi\varepsilon_0 d} \simeq 6,3eV$ ! This correspodns to a huge energy scale (remember that $1eV \sim 12000K$). Therefore we would expect that a piece of Copper at room temperature would be in a correlated state dominated by the Coulomb interaction.

This rough esimate casts some serious doubt about our global strategy. Indeed, one may legitimately worry about treating the interaction as a perturbation around the free case. Actually, the above argument is single-particle like. First, let us estimate the ratio between the potential energy and the kinetic energy, $E_{pot}/E_{Kin}$, for a given density $n$. The Coulomb energy scales as $\mathcal{V}_{\text{Coulomb}}(\bar{d}) \approx \mathcal{V}_{\text{Coulomb}}(n^{-1/d}) \sim e^2 n^{1/d}$. Therefore

$$\frac{E_{pot}}{E_{Kin}} \propto n^{-1/d}. \tag{1.13}$$

This implies that the larger the density, the more the kinetic (non-interacting) term dominates over the two-body Coulomb interaction. This estimation is a direct consequence of the Pauli principle. In the infinite density limit, the interactions are negligible and therefore this limit is a good starting point for perturbation theory.

Our piece of copper turns out to be a good metal well described by the Fermi liquid theory. Indeed, specific heat measurments are actually linear in $T$, while the susceptibility is constant. This implies that there exists an effective low-energy theory for this complicated model where interactions between the excitations (we use the term quasiparticles) are weak. This is valid in the low-temperature range such that $k_B T \ll E_{coh}$ where $E_{coh}$ denotes some energy scale which will be introduced further in the course. All the effect of the initial interactions will actually be hidden in some parameters of the Fermi liquid model such as $m^*$, $F_0$, $F_1$, $\cdots$.

The Fermi liquid theory possess a universal character in the sense that different high energy models share the same low-energy description. The relation between the high energy model and the low-energy Fermi liquid model is provided via the renormalisation group (RG) approach which connnects these models all together. We will apply this RG tool on the Anderson model [2].

## 1.3 Some elementary notions of the renormalisation group

The renormalisation group is a machinery enabling to connect high-energy degrees of freedom to low-energy ones. This is hard to implement in practice and we need to resort to a few approximation schemes. In order to obtain the low-energy observables, we need to have access to the solutions of the model at all energies. The idea of the renormalisation group is to integrate all high energy modes in order to obtain a low-energy model.

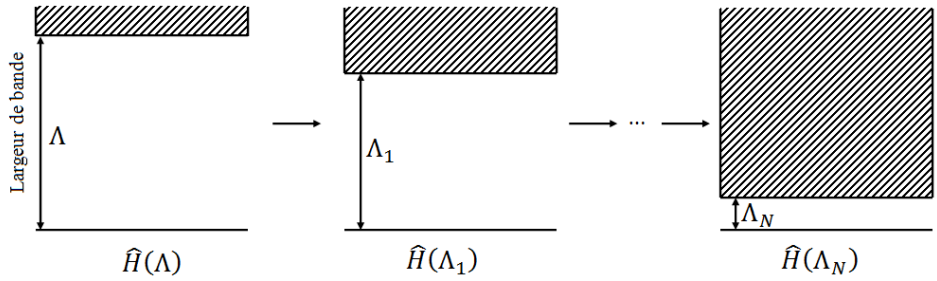


FIGURE 1.2 – Using iterative steps, the renormalisation group consists in decreasing the bandwidth by successive integration of the high-energy degrees of freedom. We stop when we arrive at fixed point given by an effective bandwidth given by $\Lambda_N$.

Let us start with $\hat{H}(\Lambda)$ where $\Lambda$ is typically the bandwidth (see Fig. 1.2). The partition function of the system reads

$$Z = \text{Tr}[e^{-\beta \hat{H}}].$$

The idea of the renormalisation group is to separate this trace into two parts : on one hand the low-energy modes ($l.e.m.$) and the high-energy modes ($h.e.m.$) :

$$Z = \text{Tr}_{l.e.m.}\text{Tr}_{h.e.m.} e^{-\beta \hat{H}(\Lambda)} = \text{Tr}_{l.e.m.} e^{-\beta \hat{H}(\Lambda_1)},$$

and to iterate such procedure until a fixed point is reached at a scale $\Lambda_N$.. Though such procedure may look simple, the catch hides in the fact that $\hat{H}(\Lambda_1)$ has in general a much more complicated and different form than

$\hat{H}(\Lambda)$ (typically n-particles processes are generated). Therefore, we are obliged to truncate some terms in $\hat{H}(\Lambda_1)$. However, at low-energy only the 2-particles processes matter (i.e are relevant) near the Fermi liquid fixed point which justifies a fortiori the truncation procedure.

If we consider the average value of an observable before renormalisation

$$\langle\hat{\Theta}\rangle = \frac{1}{Z}\mathrm{Tr}\left(\hat{\Theta}e^{-\beta\hat{H}(\Lambda)}\right),$$

after renormalisation, this average value is computed using

$$\langle\hat{\Theta}\rangle = \frac{1}{Z}\mathrm{Tr}_{l.e.m}\left(\hat{\Theta}e^{-\beta\hat{H}(\Lambda_N)}\right),$$

which is much more simple to calculate.

Obviously and fortunately, the low-energy physics of many interacting fermions does not always reduces to a Fermi liquid theory. There are other fixed points such as the Mott insulator which corresponds to an insulator driven by interactions. In one-dimension, the Fermi liquid paradigm breaks down. Technically speaking, the sucessive integration of high-energy degrees of freedom is plagued with divergences. Another paradigm, called Luttinger liquid, naturally emerges.

## 1.4 Goal of the first half of this course

The goal of the first part of this course is to calculate perturbatively (in the interactions) some physical observables. In that respect, we need to introduce the formalism of Green functions and the notion of self-energy.

# Chapitre 2

# Equilibrium single-particle Green functions

From now on, we are treating systems of $N$-particles which can be either fermions or bosons. The chemical potential is noted as $\mu$ while the temperature is $T = \frac{1}{\beta}$ (we take $k_B = 1$). We will follow the book of Bruus and Flensberg [3].

The expectation value of a quantum operator is denoted as :

$$\langle \hat{A} \rangle = \frac{1}{Z} \mathrm{Tr}(e^{-\beta \hat{H}'} \hat{A}),$$

where the partition function is defined as $Z = \mathrm{Tr}(e^{-\beta \hat{H}'})$. The Hamiltonian $\hat{H}'$ is defined as $\hat{H}' = \hat{H} - \mu \hat{N}$, i.e. in the grand-canonical ensemble. In what follows, if not stated otherwise, we will always assume such statistical ensemble, and the prime will be omitted. When possible, we will use a single index $a$ for all degrees of freedom of the system. Hence, the index $a$ can denote $\vec{k}$, $\sigma$, $\vec{x}$, ....The creation and destruction operators obey the usual relations :

$$\{\hat{c}_a, \hat{c}_b^\dagger\} = \delta_{ab} \text{ fermions} \tag{2.1}$$

$$\left[\hat{b}_a, \hat{b}_b^\dagger\right] = \delta_{ab} \text{ bosons} \tag{2.2}$$

It may be more convenient to introduce the factor $\zeta$, such that $\zeta = 1$ **for bosons** and $\zeta = -1$ **for fermions**. The commutations relations thus read

$$[\hat{\psi}_a, \hat{\psi}_b^\dagger]_\zeta = \hat{\psi}_a \hat{\psi}_b^\dagger - \zeta \hat{\psi}_b^\dagger \hat{\psi}_a = \delta_{ab}. \tag{2.3}$$

## 2.1 Definition of the Green functions

Let us introduce the following three Green functions. The retarded Green function is defined by

$$\boxed{G_{ab}^R(t - t') = -i\theta(t - t') \langle [\hat{\psi}_a(t), \hat{\psi}_b^\dagger(t')]_\zeta \rangle} \tag{2.4}$$

where the time dependence of the field operator is via the Heisenberg representation. This means

$$\hat{A}(t) = e^{i\hat{H}t} \hat{A} e^{-i\hat{H}t}.$$

Exercice Show that $G_{ab}^R(t - t')$ is indeed a function of the $t - t'$.

The second Green function is the time-ordered one Green function

$$\boxed{G_{ab}^F(t - t') = -i \langle T_t \left( \hat{\psi}_a(t) \hat{\psi}_b^\dagger(t') \right) \rangle} \tag{2.5}$$

where we introduced the time-ordered operator $T_t$ defined by

$$T_t(A(t)B(t')) = \theta(t - t')\hat{A}(t)\hat{B}(t') + \zeta_{AB}\theta(t' - t)\hat{B}(t')\hat{A}(t),$$

where $\zeta_{AB} = -1$ if $\hat{A}$ and $\hat{B}$ are fermionic operators and $+1$ if they are bosonic operators.

Finally the third Green function we want to introduce is called the Matsubara Green function which is defined in imaginary time. Like complex numbers, the imaginary time or Euclidian time is a technical trick where time and frequency are imaginary. We will see the advantages of such trick later. Let us define the imaginary time evolution by analytic continuation as

$$\hat{A}(\tau) = e^{\hat{H}\tau}\hat{A}e^{-\hat{H}\tau},\ \tau \in [0, \beta]. \tag{2.6}$$

Please pay attention that

$$\hat{A}(\tau)^\dagger = \hat{A}^\dagger(-\tau) \neq \hat{A}^\dagger(\tau).$$

The Matsubara Green function is then defined by :

$$\boxed{G^M_{ab}(\tau - \tau') = -\left\langle T_\tau \left(\hat{\psi}_a(\tau)\hat{\psi}^\dagger_b(\tau')\right)\right\rangle,} \tag{2.7}$$

where as previously, $T_\tau[\hat{A}(\tau)\hat{B}(\tau')] = \hat{A}(\tau)\hat{B}(\tau')$ if $\tau > \tau'$, and $T_\tau[\hat{A}(\tau)\hat{B}(\tau')] = \zeta_{AB}\hat{B}(\tau')\hat{A}(\tau)$ if $\tau < \tau'$. Note that $\tau \in [0, \beta]$ garenties the convergence of the Green function $G^M_{ab}(\tau)$. One may wonder what is the use of such Green function. We will come back to it later when analyzing its properties in details. In short, define the correlator $C_{AB}(t, t') = -\langle A(t)B(t')\rangle$ such that $C^R_{AB} = i\theta(t-t')(C_{AB}(t, t') - \zeta C_{BA}(t', t))$. Coming back to the definition of the expectation values,

$$C_{AB}(t, t') = -\frac{1}{Z}Tr\left(e^{-\beta H}A(t)B(t')\right) = -\frac{1}{Z}Tr\left(e^{-\beta H}e^{iHt}Ae^{-iH(t-t')}Be^{-iHt'}\right) \tag{2.8}$$

$$= -\frac{1}{Z}Tr\left(e^{-\beta H}e^{H\tau}Ae^{-H(\tau-\tau')}Be^{-H\tau'}\right). \tag{2.9}$$

We have used the Heisenberg representation and assumed the Hamiltonian $H$ to be time-independent. The main advantage of this formulation can be seen in the later expression where the density operator and the time evolution can be treated on an equal footing. Therefore such formulation will be quite convenient to deal with finite temperature Green functions and the calculations of finite T observables.

At $T = 0$, $G^F$ can be developed using perturbation theory and Feynman diagrams while $G^R$ cannot. At $T \neq 0$, $G^M$ can also be computed using perturbation theory and Feynman diagrams while $G^R$ cannot. $G^R$ will be obtained by an analytical continuation of $G^M$. Moreoevr, the function $\rho_{ab}$ will be derived from $G^R$ as follows

$$\boxed{\rho_{ab} = -\frac{1}{\pi}\Im G^R_{ab}(\omega).} \tag{2.10}$$

The spectral function encodes all the information on the excitations spectrum of the system.

Finally, it is worth emphasizing that the retarded Green function is the most physical one since it naturally emerges in linear response theory as the response to a perturbation done earlier in time. However, as we just saw, the latter can not be computed directly and we need tu use the other Green functions as some intermediate steps to obtain it though these other Green functions are not physical.

## 2.2 Properties of the Matsubara Green function

### 2.2.1 Periodicity and Fourier series

The Matsubara Green function is a function of the difference between the imaginary times $(\tau - \tau')$. Therefore if $0 \leq \tau, \tau' \leq \beta$, we have $-\beta \leq \tau - \tau' \leq \beta$, which implies $G^M_{ab}$ varies over an interval of width $2\beta$. We can then extend $G^M_{ab}$ for real values of $\tau - \tau'$ by continuity and using the $2\beta$ periodicity (see FIG. 2.1). The function $G^M_{ab}$ is thus $2\beta$ periodic in general

$$G^M_{ab}(\tau + 2\beta) = G^M_{ab}(\tau). \tag{2.11}$$

A consequence of this periodicity is the ability to expand it in Fourier series.

Another property of the Matsubara Green function is the following :

$$G^M_{ab}(\tau + \beta) = \zeta G^M_{ab}(\tau), \tag{2.12}$$

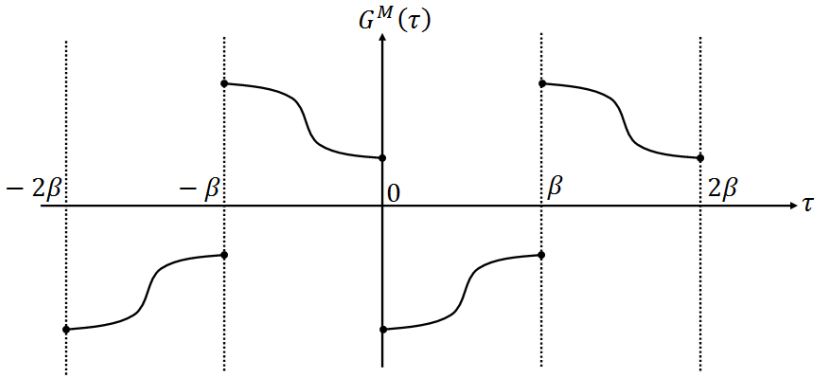


FIGURE 2.1 – The Green function $G^M_{ab}(\tau)$ has a $2\beta$ periodicity, and according to the nature of the particules (fermionic or bosonic), the Matsubara Green function is actually $\beta$-antiperiodic (fermions) or $\beta$-periodic (bosons)

implying a periodicity $\beta$ for bosons and an antiperiodicity $\beta$ for fermions. To show this property, let us assume $\tau \in [-\beta, 0]$, such that $\tau + \beta > 0$

$$G^M_{ab}(\tau+\beta) = -\frac{1}{Z}\mathrm{Tr}\left(e^{-\beta\hat{H}}T_\tau(\hat{\psi}_a(\tau+\beta)\hat{\psi}^\dagger_b(0))\right).$$

With these conditions on $\tau$ and $\beta$, we can suppress the time-ordering operator and write

$$G^M_{ab}(\tau+\beta) = -\frac{1}{Z}\mathrm{Tr}\left(e^{-\beta\hat{H}}e^{(\tau+\beta)\hat{H}}\hat{\psi}_a e^{-(\tau+\beta)\hat{H}}\hat{\psi}^\dagger_b\right).$$

This expression can be simplified

$$G^M_{ab}(\tau+\beta) = -\frac{1}{Z}\mathrm{Tr}\left(e^{\tau\hat{H}}\hat{\psi}_a e^{-(\tau+\beta)\hat{H}}\hat{\psi}^\dagger_b\right),$$

and using the property of the trace, we get

$$G^M_{ab}(\tau+\beta) = -\frac{1}{Z}\mathrm{Tr}\left(e^{-\beta\hat{H}}\hat{\psi}^\dagger_b e^{\tau\hat{H}}\hat{\psi}_a e^{-\tau\hat{H}}\right),$$

where we can identify $\hat{\psi}^\dagger_b(0)$ and $\hat{\psi}_a(\tau)$. This thus allows us to rewrite the expression as

$$G^M_{ab}(\tau+\beta) = -\frac{\zeta}{Z}\mathrm{Tr}\left[e^{-\beta\hat{H}}T_\tau(\hat{\psi}_a(\tau)\hat{\psi}^\dagger_b(0))\right] = \zeta G^M_{ab}(\tau).$$

We can perform a similar calculation if $\tau > 0$. Therefore, this shows the property of periodicty or antiperiodicity of $G^M_{ab}(\tau)$.

The Matsubara Green function can be expanded in Fourier series as

$$G^M_{ab}(\tau) = \frac{1}{\beta}\sum_{\omega_n} e^{-i\omega_n\tau}G^M_{ab}(i\omega_n), \tag{2.13}$$

where the Matsubara frequencies $\omega_n$ are given by

$$e^{i\omega_n\beta} = \zeta. \tag{2.14}$$

We thus have $\omega_n = \pi T(2n+1)$ for fermions and $\omega_n = \pi T 2n$ for bosons.

We can reverse the Eq. (2.13), to obtain

$$G^M_{ab}(i\omega_n) = \int_0^\beta d\tau G^M_{ab}(\tau)e^{i\omega_n\tau}. \tag{2.15}$$

Exercice Show that

$$G^M_{ab}(i\omega_n) = \int_{-\beta/2}^{\beta/2} d\tau G^M_{ab}(\tau)e^{i\omega_n\tau}.$$

### 2.2.2 Discontinuity in $\tau = 0$ and particle number

As the figure 2.1 may indicate, the Matsubara Green function has a singular behavior in $\tau = 0$. One can show that

$$G^M_{ab}(0^+) - G^M_{ab}(0^-) = -\delta_{ab}. \tag{2.16}$$

Indeed,

$$\langle T_\tau \hat{\psi}_a(0^+)\hat{\psi}^\dagger_b(0)\rangle = \langle \hat{\psi}_a\hat{\psi}^\dagger_b\rangle\,,\ \langle T_\tau \hat{\psi}_a(0^-)\hat{\psi}_b(0)\rangle = \zeta\,\langle \hat{\psi}^\dagger_b\hat{\psi}_a\rangle\,.$$

Substracting these two expressions, we obtain

$$\begin{aligned} G^M_{ab}(0^+) - G^M_{ab}(0^-) &= -[\langle \hat{\psi}_a\hat{\psi}^\dagger_b\rangle - \zeta\,\langle \hat{\psi}^\dagger_b\hat{\psi}_a\rangle] \\ &= -\langle \hat{\psi}_a\hat{\psi}^\dagger_b - \zeta\hat{\psi}^\dagger_b\hat{\psi}_a\rangle \\ &= -\delta_{ab}. \end{aligned}$$

Another important property of the Matsubara Green function is its large frequency behavior :

$$\lim_{\omega_n\to+\infty} G^M_{ab}(i\omega_n) = \frac{\delta_{ab}}{i\omega_n}. \tag{2.17}$$

For fermions, the number of particules (electrons) in the state $a$ is given by

$$n_a = \langle \hat{\psi}^\dagger_a\hat{\psi}_a\rangle = G^M_{aa}(0^-),$$

(Similarly the number of particles with momentum $k$ is given by $G^M_k(0^-)$), and conversely, the number of anti-particles (holes) is given by

$$n_a - 1 = -\langle \hat{\psi}_a\hat{\psi}^\dagger_a\rangle = G^M_{aa}(0^+).$$

## 2.3 Free fermions

We are interested here in free fermions described by a quadratic Hamiltonian.

### 2.3.1 Single-level Hamiltonian (see exercice sheet)

Let us consider the simplest possible case, a single level Hamiltonian described by

$$\hat{H} = \varepsilon\hat{c}^\dagger\hat{c},$$

Exercice Compute the following Green functions $G^M(\tau)$, $G^M(i\omega_n)$ and $G^R(\omega)$

The Matsubara Green function is given by

$$G^M(\tau,\tau') = -\langle T_\tau(\hat{c}(\tau)\hat{c}^\dagger(\tau'))\rangle\,.$$

The evolution of an operator in imaginary time is given by

$$\hat{A}(\tau) = e^{\hat{H}\tau}\hat{A}e^{-\hat{H}\tau},$$

and therefore the operator $\hat{c}(\tau)$ satisfies the following differential equation

$$\partial_\tau\hat{c}(\tau) = e^{\hat{H}\tau}[\hat{H},\hat{c}]e^{-\hat{H}\tau}.$$

Using the anticommutation relations, we thus obtain $\partial_\tau\hat{c}(\tau) = -\varepsilon\hat{c}(\tau)$, and therefore $\hat{c}(\tau) = e^{-\varepsilon\tau}c$. The Hilbert space of this system reduces to the states $|0\rangle$ and $|1\rangle$ with 0 or 1 particles respectively. The eigenvalues of $\hat{H}$ are 0 and $\varepsilon$ associated with these above eigenstates.

With the expression of $\hat{c}(\tau)$, we can compute direcly the Matsubara Green function. For $\tau > 0$, we have

$$G^M(\tau) = G^M(\tau,0) = -\langle \hat{c}(\tau)\hat{c}^\dagger(0)\rangle = -e^{-\varepsilon\tau}\,\langle \hat{c}\hat{c}^\dagger\rangle\,.$$

The expectation value of the number operator reads

$$\langle \hat{c}\hat{c}^\dagger \rangle = 1 - \langle \hat{c}^\dagger \hat{c} \rangle = \frac{1}{1+e^{-\beta\varepsilon}},$$

and we thus get

$$G^M(\tau) = \frac{-e^{-\varepsilon\tau}}{1+e^{-\beta\varepsilon}} \ \tau > 0,$$

and using fermionic anticommutation relations, we infer for $\tau < 0$ that

$$G^M(\tau) = \frac{e^{-\varepsilon\tau}}{1+e^{\beta\varepsilon}}.$$

This function is shown in Fig. 2.2.

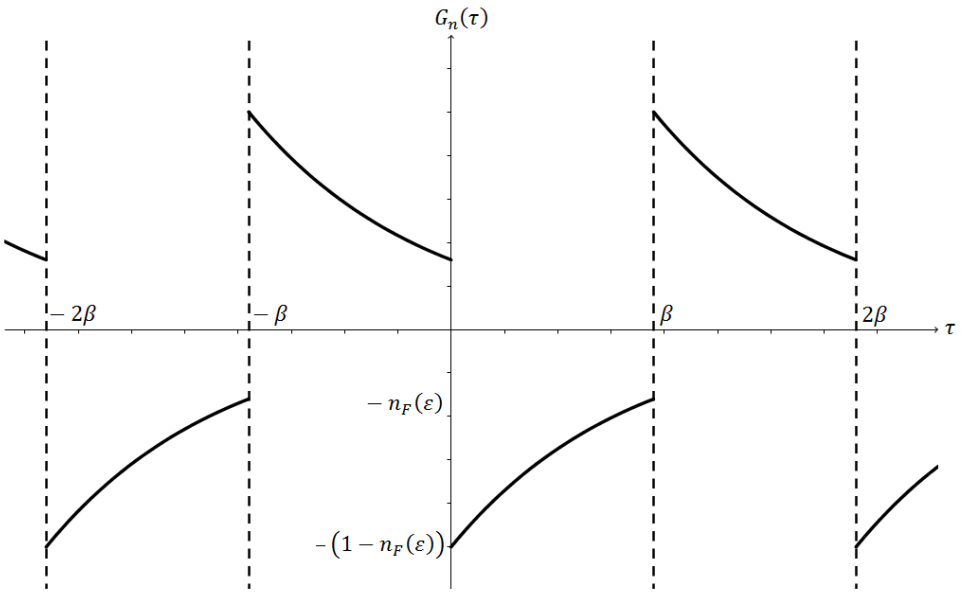


FIGURE 2.2 – Matsubara Green function for free fermions.

Furthermore, the value of $G^M(\tau)$ in $0^+$ and $\beta^-$ take the following simple expressions

$$G^M(\tau = 0^+) = -(1 - n_F(\varepsilon)) \ G^M(\tau = \beta^-) = -n_F(\varepsilon),$$

where $n_F$ is the Fermi Dirac distribution function.

Let us now compute the Fourier transform $G^M(i\omega_n)$ of $G^M(\tau)$ :

$$\begin{aligned} G^M(i\omega_n) &= \int_0^\beta d\tau G^M(\tau) e^{i\omega_n \tau} = \int_0^\beta d\tau \frac{-e^{-\varepsilon\tau}}{1+e^{-\beta\varepsilon}} e^{i\omega_n \varepsilon} \\ &= -\frac{1}{1+e^{-\beta\varepsilon}} \int_0^\beta e^{\tau(i\omega_n - \varepsilon)} = -\frac{1}{1+e^{-\beta\varepsilon}} \left[ \frac{e^{\beta(i\omega_n - \varepsilon)} - 1}{i\omega_n - \varepsilon} \right]. \end{aligned}$$

Using the definition of the Matsubara frequencies in (2.14), we can simplify this ersult to simply write

$$G^M(i\omega_n) = \frac{1}{i\omega_n - \varepsilon}$$

Let us now compute the retarded Greenfunction $G^R(t)$ which reads

$$G^R(t) = -i\theta(t) \left\langle [\hat{c}(t), \hat{c}^\dagger]_\zeta \right\rangle.$$

The time evolution of $\hat{c}$ can be determined following the same steps as for the imaginary time. We thus get $\partial_t \hat{c}(t) = -i\varepsilon\hat{c}(t)$, and therefore $\hat{c}(t) = e^{-i\varepsilon t}\hat{c}$ (which corresponds to the analytic continuation of $\hat{c}(\tau)$). We obtain

$$G^R(t) = -i\theta(t)e^{-i\varepsilon t}\langle\{\hat{c}, \hat{c}^\dagger\}\rangle = -i\theta(t)e^{-i\varepsilon t}.$$

In order to determine $G^R(\omega)$, we take the Fourier transform of the previous expression

$$G^R(\omega) = \int_{-\infty}^{+\infty} dt G^R(t)e^{i\omega t} = -i\int_0^{+\infty} e^{i(\omega-\varepsilon)t}. \tag{2.18}$$

This integral being divergent, we introduce an infinitesimal regulator $i\eta$ (with $\eta > 0$) such that

$$\begin{aligned} G^R(\omega) &= \lim_{\eta\to 0^+} -i\int_0^{+\infty} e^{i(\omega-\varepsilon)t}e^{-\eta t} \\ &= \lim_{\eta\to 0^+} \frac{1}{i\eta + \omega - \varepsilon}. \end{aligned}$$

The retarded Green function possesses a pole in the lower half-plane. Notice that this is a general property. Indeed, suppose we start from the Fourier transform of

$$G^R(t) = \int_{-\infty}^{+\infty} \frac{d\omega}{2\pi} G^R(\omega)e^{-i\omega t},$$

and extend $\omega$ into the complex plane, namely let us consider $G^R(\omega) \longrightarrow G^R(z)$. We assume $G^R(z)$ to be analytical in the upper half complex plane. For $t > 0$, we need to close the contour over the lower half plane to make the integral convergent. Therefore, $G^R(t)$ is dominated by the zeroes of $G^R(z)$. Instead, if $t < 0$, we need to close the contour in the upper half plane and therefore $G^R(t < 0) = 0$. This implies that $G^R(t) \propto \theta(t)$. We thus have an equivalence between the following two properties

$$G^R(t) \propto \theta(t) \iff G^R(z) \text{ analytical in the upper halfplane.} \tag{2.19}$$

Coming back to the retarded Green function, The retarded and Matsubara Green functions are related within each other using a simple analytical continuation

$$\boxed{G^M(i\omega_n \to \omega + i0^+) = G^R(\omega)}.$$

The previous relation between $G^R(\omega)$ and $G^M(i\omega_n)$ is also valid for bosons and is actually quite general and relies on the existence of a spectral decomposition.

The density of states $\rho(\omega)$ is obtained via $\rho(\omega) = -\frac{1}{\pi}\Im G^R(\omega)$. Using $\frac{1}{x+i0^+} = \mathcal{P}\mathcal{P}\frac{1}{x} - i\pi\delta(x)$, we simply get

$$\rho(\omega) = \delta(\omega - \varepsilon).$$

### 2.3.2 Diagonalisation and relations with the Green functions

We treated above the case of a single level. Let us extend it to free fermions described by a general quadratic Hamiltonian

$$\hat{H} = \sum_{\alpha\beta} \hat{c}^\dagger_\alpha h_{\alpha\beta}\hat{c}_\beta. \tag{2.20}$$

$h$ is a Hermitian matrix (i.e. $h^*_{\beta\alpha} = h_{\alpha\beta}$). We can find some unitary transform $h = U\Lambda U^\dagger$, where $U$ is some unitary matrix ($UU^\dagger = U^\dagger U = 1$) and where $\Lambda$ is a diagonal matrix with eigenvalues noted $\lambda_i$. We introduce the notation

$$\vec{\hat{c}} = \begin{pmatrix} \vdots \\ \hat{c}_\alpha \\ \vdots \end{pmatrix},$$

Under such unitary transform, we define new vectors $\vec{\hat{c}}' = U^\dagger\vec{\hat{c}}$ or in composants $\vec{\hat{c}}'^\dagger_\beta = \vec{\hat{c}}_{\beta'}U_{\beta'\beta}$.

Exercice **Check these new operators $\hat{c}'$ satisfy the usual anticommutation relations.**

The Hamiltonian in Eq. (2.16) can be thus written as

$$\hat{H} = \sum_{\alpha} \lambda_\alpha \hat{c}'^{\dagger}_{\alpha} \hat{c}'_{\alpha}.$$

In this form, the Hamiltonian is a simple extension of the single level Hamiltonian we dealt in Sec. 2.3.1.

The Matsubara Green function $G^M_{\alpha\beta}(\tau)$ is defined by

$$G^M_{\alpha\beta}(\tau) = -\left\langle T_\tau \hat{c}_\alpha(\tau) \hat{c}^\dagger_\beta(0) \right\rangle .$$

To calculate this Green function, we then use the unitary transform

$$G^M_{\alpha\beta}(\tau) = -\left\langle T_\tau \hat{c}'_{\alpha'}(\tau) \hat{c}'^{\dagger}_{\beta'}(0) \right\rangle U_{\alpha\alpha'} U^\dagger_{\beta'\beta},$$

where the Einstein convention is used (i.e. repetition of two indices imply their summation). We calculated this expectation value previously, namely

$$\langle T_\tau \hat{c}'_{\alpha'}(\tau) \hat{c}'^{\dagger}_{\beta'}(0) \rangle = \delta_{\alpha'\beta'} \frac{-e^{-\lambda_{\alpha'}\tau}}{1+e^{-\beta\lambda_{\alpha'}}}, \quad \text{for} \quad \tau > 0.$$

The Fourier transform of this expression gives

$$G^M_{\alpha\beta}(i\omega_n) = U_{\alpha\alpha'} \frac{1}{i\omega_n - \lambda_{\alpha'}} U^\dagger_{\alpha'\beta}, \tag{2.21}$$

which can be compactly written as follows

$$G^M_{\alpha\beta}(i\omega_n) = \left( \frac{1}{i\omega_n - h} \right)_{\alpha\beta}.$$

The last line comes simply from $h = U\Lambda U^\dagger$ and therefore $U f(\Lambda) U^\dagger = f(h)$ for any function $f$ which can be expanded in Taylor series. The quantity $R = \frac{1}{\omega - h}$ corresponds to the analytic continuation of the previous expression which is called the resolvant in the literature. It has some properties which have been developed for the studies of scattering problems in the fifties.

### 2.3.3 The resonant level model

Let us consider now the case of a state $|d\rangle$ coupled to a a large number of states labeled by $|k\rangle$. Such a situation is described by the following Hamiltonian

$$\hat{H} = \varepsilon_d \hat{d}^\dagger \hat{d} + \sum_{\vec{k}} \varepsilon_k \hat{c}^\dagger_k \hat{c}_k + \frac{t}{\sqrt{V}} \sum_k (\hat{c}^\dagger_k \hat{d} + \text{h.c.}). \tag{2.22}$$

Typically, the state labeled by $d$ indicates a quantum dot or some d orbital of a magnetic atom coupled to a Fermi sea. Our goal is to obtain the spectral function $\rho(\omega)$ of such system. Notice that we are still dealing with a non-interacting Hamiltonian and therefore this is clearly a oversimplified description of the reality. However, it still embodies a large set of situations essentially because of the Fermi liquid picture and renormalization group arguments we developed in the introduction. We will come back to this point later in the course.

To start with, let us compute the Matsubara Green function $G^M_d(i\omega_n)$ defined in this case as

$$G^M_d(\tau) = -\left\langle T_\tau \hat{d}(\tau) \hat{d}^\dagger(0) \right\rangle .$$

Using previous notations, we can write our Hamiltonian in terms of a matrix $h$ of the following form

$$h = \begin{pmatrix} \varepsilon_d & t/\sqrt{V} & \cdots & t/\sqrt{V} \\ t/\sqrt{V} & \varepsilon_{k_1} & & 0 \\ \vdots & & \ddots & \\ t/\sqrt{V} & 0 & & \varepsilon_{k_N} \end{pmatrix}.$$

Remind that for a block-matrix of the form

$$\begin{pmatrix} A & B \\ C & D \end{pmatrix},$$

assuming it can be inverted, the inverse of the first block (in the same position as $A$) reads $(A - BD^{-1}C)^{-1}$. In our basis, this term corresponds to the diagonal term coupling the state $d$ with itself. Indeed, we can identify $A = \varepsilon_d$, $B = \left(t/\sqrt{V}, \cdots, t/\sqrt{V}\right)$, $C = B^t$ and

$$D = \begin{pmatrix} \varepsilon_{k_1} & & 0 \\ & \ddots & \\ 0 & & \varepsilon_{k_N} \end{pmatrix}.$$

Therefore

$$\begin{aligned} A - BD^{-1}C &= \varepsilon_d - \frac{t}{\sqrt{V}} \begin{pmatrix} 1 & \cdots & 1 \end{pmatrix} \begin{pmatrix} 1/\varepsilon_{k_1} & & 0 \\ & \ddots & \\ 0 & & 1/\varepsilon_{k_N} \end{pmatrix} \begin{pmatrix} 1 \\ \vdots \\ 1 \end{pmatrix} \\ &= \varepsilon_d - \frac{t^2}{V} \sum_k \frac{1}{\varepsilon_k}. \end{aligned}$$

We have previously seen that $G^M_{\alpha\beta}(i\omega_n)$ is given by the inverse of the matrix $i\omega_n - h$, and therefore

$$\begin{aligned} G^M_d(i\omega_n) &= (i\omega_n - M)^{-1} = \left( i\omega_n - \varepsilon_d - \sum_k \frac{t^2}{V} \frac{1}{i\omega_n - \varepsilon_k} \right)^{-1} \\ &= \frac{1}{i\omega_n - \varepsilon_d - \frac{t^2}{V} \sum_k \frac{1}{i\omega_n - \varepsilon_k}}. \end{aligned}$$

By analytic continuation, we obtain the retarded Green function

$$G^R_d(\omega) = \frac{1}{\omega - \varepsilon_d + i0^+ - \frac{t^2}{V} \sum_k \frac{1}{\omega - \varepsilon_k + i0^+}}.$$

We introduce the so-called **self-energy** $\Sigma = \frac{t^2}{V} \sum_k \frac{1}{i\omega_n - \varepsilon_k + i0^+}$. This function of $\omega$ is *a priori* complex, and we note

$$\Sigma = \Sigma_1 + i\Sigma_2 = \Sigma' + i\Sigma''.$$

The real part of the self-energy is given by the principal part of $\Sigma$

$$\Sigma_1 = \frac{t^2}{V} \sum_k \mathcal{P}\mathcal{P} \frac{1}{\omega - \varepsilon_k},$$

while the imaginary part of $\sigma$ is given by

$$\Sigma_2 = -\frac{\pi t^2}{V} \sum_k \delta(\omega - \varepsilon_k).$$

The discrete sums being difficult to calculate in general, we take the continuum limit to calculate $\Sigma_1$ and $\Sigma_2$. We therefore replace the discrete sum by an integral in energy :

$$\Sigma_1 = t^2 \nu_0 \mathcal{P}\mathcal{P} \int_{-D}^{D} d\varepsilon \frac{1}{\omega - \varepsilon},$$

where $\nu_0$ is the density of states at the Fermi level and $D$ the bandwidth.

To calculate this integral, we cut it into two pieces before and after the discontinuity and introduce some infinitesimal energy cut-off $\delta$. On the right side, we get

$$\int_{\omega+\delta}^{D} d\varepsilon \frac{1}{\omega - \varepsilon} = -\int_{\delta}^{D-\omega} \frac{d\varepsilon}{\omega} = -\ln \frac{D - \omega}{\delta},$$

while on the left side, we have

$$\int_{-D}^{\omega-\delta} d\varepsilon \frac{1}{\omega-\varepsilon} = \int_{-\omega+\delta}^{D} d\varepsilon \frac{1}{\omega+\varepsilon} = \ln \frac{D+\omega}{\delta}.$$

Gathering both pieces,

$$\Sigma_1 = t^2\nu_0 \left( -\ln\left(\frac{D-\omega}{\delta}\right) + \ln\left(\frac{D+\omega}{\delta}\right)\right) = t^2\nu_0 \ln \frac{D+\omega}{D-\omega}.$$

In the limit $D \to \infty$ (the large band limit), this contribution to the self-emergy tends toward 0. This is typically the case if we are interested in physical processes occuring in some range of energy $\Delta E \ll D$ around the finite level. Let us now evaluate $\Sigma_2$ which reads

$$\Sigma_2 = -\pi t^2 \nu_0 \int d\varepsilon \delta(\omega-\varepsilon) = -\pi t^2 \nu_0 \equiv -\Gamma.$$

where we introduce the energy $\Gamma = \pi t^2 \nu_0$ that corresponds to the finite energy width of the level.

The retarded Green function is finally given in the large bandwidth as

$$G_d^R(\omega) = \frac{1}{\omega - \varepsilon_d + i\Gamma}. \tag{2.23}$$

The spectral function of the d-level (also called the local density of states) thus reads

$$\rho_d(\omega) = -\frac{1}{\pi}\Im G_d^R(\omega) = \frac{1}{\pi}\frac{\Gamma}{(\omega-\varepsilon_d)^2+\Gamma^2}.$$

This function is normalized to 1. $\rho_d$ corresponds to a Lorentzian distribution of width $\Gamma$ centered around the energy of the isolated level described by $|d\rangle$. Consequently, the coupling between a localized level and a continuum of states entails a broadening of the delta peak of the isolated states.

Let us come back to the retarded Green function of the d-level :

$$G_d^R(t) = \int_{-\infty}^{+\infty} \frac{d\omega}{2\pi} \frac{e^{-i\omega t}}{\omega - \varepsilon_d + i\Gamma}.$$

The calculation of this integral can be achieved using the residue theorem. As above we have $G_d^R(t<0) = 0$ as it should be. However for $t > 0$, the pole in the lower half-plane provides a contribution and we obtain

$$G_d^R(t) = -i\theta(t) e^{-i\varepsilon_d t} e^{-\Gamma t}. \tag{2.24}$$

$G_d^R(t)$ can be interpreted as the probability amplitude for an electron in the resonant d-level at $t = 0$ to remain in this state at time $t$. Indeed, we can write

$$G_d^R(t) = \langle 0|\hat{d}\hat{U}(t)\hat{d}^\dagger|0\rangle,$$

where $\hat{U}(t)$ denotes the evolution operator $e^{-i\hat{H}}$. We can recognize the Fermi Golden rule. Therefore, the probability for the electron to remain in the state $|d\rangle$ is given by

$$P_d(t) = |G_d^R(t)|^2 = e^{-2\Gamma t} = e^{-t/\tau},$$

where $\tau = \frac{1}{2\Gamma}$ corresponds to the characterisic emission time.

## 2.4 Spectral representation

### 2.4.1 Lehmann representation

We have expressed in the previous section the single-particle Green function. Let us extend them to interacting particles. Before demonstrating their expression, we summarized them in the following array for fermions

| | Free fermion | General case |
|---|---|---|
| $G^M(i\omega_n)$ | $\frac{1}{i\omega_n-\varepsilon}$ | $\int d\omega' \frac{\rho_{\alpha\beta}(\omega')}{i\omega_n-\omega'}$ |
| $G^M(\tau)$ | $-\frac{e^{-\varepsilon\tau}}{1+e^{-\beta\varepsilon}}$ | $\int d\omega' \rho_{\alpha\beta}(\omega') \frac{-e^{-\omega'\tau}}{1+e^{-\beta\omega'}}$ |
| $G^R(t)$ | $-i\theta(t)e^{-i\varepsilon t}$ | $\int d\omega' \rho_{\alpha\beta}(\omega') e^{-i\omega' t}$ |
| $\rho_{\alpha\beta}(\omega)$ | $\delta(\omega-\varepsilon)$ | $\rho_{\alpha\beta}(\omega)$ |

The following relations are general (whatever the nature of particles even in presence of interactions)

$$G^M_{\alpha\beta}(i\omega_n) = \int_{-\infty}^{+\infty} d\varepsilon \frac{\rho_{\alpha\beta}(\varepsilon)}{i\omega_n-\varepsilon}, \tag{2.25}$$

$$G^R_{\alpha\beta}(\omega) = \int_{-\infty}^{+\infty} d\varepsilon \frac{\rho_{\alpha\beta}(\varepsilon)}{\omega-\varepsilon+i0^+}. \tag{2.26}$$

As will be show further these definitions and relations rely on the existence of an Hilbert space. FRom the Lehmann representation we define and write the spectral function (or density of states) as

$$\rho_{\alpha\beta}(\omega) = \frac{1}{Z}\sum_{A,B} e^{\beta\mu N_A}(e^{-\beta E_A} - \zeta_\psi e^{-\beta(E_B+\mu)}) \times \langle A|\hat{c}_\alpha|B\rangle \langle B|\hat{c}^\dagger_\beta|A\rangle \delta(\omega+\mu+E_A-E_B), \tag{2.27}$$

where $|A\rangle$ and $|B\rangle$ are eigenstates of $\hat{H}-\mu\hat{N}$ with eigenvalues

$$E'_A = E_A - \mu N_A,\ E'_B = E_B - \mu(N_A+1).$$

If we instead use the energy eigenvalues of $H'$, Eq. (2.27) simply reads :

$$\rho_{\alpha\beta}(\omega) = \frac{1}{Z}\sum_{A,B} (e^{-\beta E'_A} - \zeta_\psi e^{-\beta E'_B}) \times \langle A|\hat{c}_\alpha|B\rangle \langle B|\hat{c}^\dagger_\beta|A\rangle \delta(\omega+E'_A-E'_B), \tag{2.28}$$

Note however that $\rho_{\alpha\beta}(\omega)$ being a probability density, it is normalized and satisfies

$$\int_{-\infty}^{+\infty} \rho_{\alpha\beta}(\omega)d\omega = \delta_{\alpha\beta}.$$

Exercice Show the above property starting from Eq. (2.28)

When $\alpha$ and $\beta$ correspond to single-particles eigenstates, $\langle B|\hat{c}^\dagger_\beta|A\rangle$ is different from 0 iff $E_B = E_A+\varepsilon_\beta$ in which case we can replace the Dirac distribution in Eq. (2.27) by $\delta(\omega+\mu-\varepsilon_\beta)$. We thus obtain the following expression for the retarded Green function

$$G^R_{\alpha\beta}(t) = \delta_{\alpha\beta}(-i\theta(t)e^{-i(\varepsilon_\alpha-\mu)t}),$$

indicating quantum coherence.

To demonstrate (2.25) and (2.26), we consider first the retarded Green function

$$G^R_{ab}(t-t') = -i\theta(t-t')\langle[\hat{\psi}_\alpha(t), \hat{\psi}^\dagger_\beta(t')]_{\zeta_\psi}\rangle,$$

and define the following two other Green functions

$$G^>_{\alpha\beta}(t-t') = -i\langle\hat{\psi}_\alpha(t)\hat{\psi}^\dagger_\beta(t')\rangle$$
$$G^<_{\alpha\beta}(t-t') = -i\zeta_\psi\langle\hat{\psi}^\dagger_\beta(t')\hat{\psi}_\alpha(t)\rangle,$$

which are called the greater and lesser Green functions respectively. These Green functions will play a role later on when we will discuss transport properties. The retarded Green function can be thus expressed as

$$G^R_{\alpha\beta}(t-t') = \theta(t-t')(G^>_{\alpha\beta}(t-t') - G^<_{\alpha\beta}(t-t')).$$

I remind that $\langle\cdots\rangle$ is defined by $\frac{1}{Z}\mathrm{Tr}(e^{-\beta\hat{H}'}\cdots)$, where $\hat{H}'=\hat{H}-\mu\hat{N}$. Let us introduce the eigenstates of $\hat{H}'$ noted $|A\rangle$ and $|B\rangle$. We have for $G^{>}$

$$G^{>}_{\alpha\beta}(t-t')=-\frac{i}{Z}\mathrm{Tr}(e^{-\beta\hat{H}'}\hat{\psi}_\alpha(t)\hat{\psi}_\beta(t')).$$

Introducing two resolutions of the identity in this expression and using the time evolution of $\hat{\psi}_\alpha(t)=e^{i\hat{H}'t}\hat{\psi}_\alpha e^{-i\hat{H}'t}$, we can write

$$G^{>}_{\alpha\beta}(t-t')=-\frac{i}{Z}\sum_{A,B}e^{-\beta E'_A}\,\langle A|\hat{\psi}_\alpha|B\rangle\,\langle B|\hat{\psi}^\dagger_\beta|A\rangle\,e^{i(E'_A-E'_B)(t-t')}.$$

Using a similar reasoning we can also express $G^{<}_{\alpha\beta}$

$$G^{<}_{\alpha\beta}(t-t')=-\frac{i\zeta_\psi}{Z}\sum_{A,B}e^{-\beta E'_B}\,\langle A|\hat{\psi}_\alpha|B\rangle\,\langle B|\hat{\psi}^\dagger_\beta|A\rangle\,e^{i(E'_A-E'_B)(t-t')}.$$

Finaly the retarded Green function reads

$$G^{R}_{\alpha\beta}(t)=\frac{1}{Z}\sum_{A,B}\langle A|\hat{\psi}_\alpha|B\rangle\,\langle B|\hat{\psi}^\dagger_\beta|A\rangle\,(-i)\theta(t)e^{i(E'_A-E'_B)t}(e^{-\beta E'_A}-\zeta_\psi e^{-\beta E'_B}).$$

By Fourier transforming it, we obtain the energy dependence of the retarded Green function as

$$G^{R}_{\alpha\beta}(\omega)=\frac{1}{Z}\sum_{A,B}\frac{\langle A|\hat{\psi}_\alpha|B\rangle\,\langle B|\hat{\psi}^\dagger_\beta|A\rangle}{\omega+E'_A-E'_B+i0^+}(e^{-\beta E'_A}-\zeta_\psi e^{-\beta E'_B}).$$

Using the property that

$$\frac{1}{\omega+E+i0^+}=PP\left(\frac{1}{\omega+E}\right)-i\pi\delta(\omega+E),$$

we introduce the spectral function (i.e. density of states) as

$$\boxed{\rho_{\alpha\beta}(\varepsilon)=\tfrac{1}{Z}\textstyle\sum_{A,B}\langle A|\hat{\psi}_\alpha|B\rangle\,\langle B|\hat{\psi}^\dagger_\beta|A\rangle\,(e^{-\beta E'_A}-\zeta_\psi e^{-\beta E'_B})\delta(\epsilon+E'_A-E'_B)}. \tag{2.29}$$

With this identification of the spectral function, we can thus write the retarded Green function as

$$G^{R}_{\alpha\beta}(\omega)=\int d\varepsilon\frac{\rho_{\alpha\beta}(\varepsilon)}{\omega-\varepsilon+i0^+}.$$

This explictly demonstration the expression (2.26) for the retarded Green function from the identification of the spectral function in Eq. (2.29).

Note that for fermions, $\rho_{\alpha\alpha}$ is real and satisfies $\rho_{\alpha\alpha}(\varepsilon)\geq 0$.

Concerning the Matsubara Green function, we have

$$G^{M}_{\alpha\beta}(\tau)=-\frac{1}{Z}\sum_{A,B}e^{-\beta E'_A}\,\langle A|\hat{\psi}_\alpha|B\rangle\,\langle B|\hat{\psi}^\dagger_\beta|A\rangle\,e^{(E'_A-E'_B)\tau},$$

and its Fourier transform as

$$\begin{aligned}
G^{M}_{\alpha\beta}(i\omega_n) &= \int_0^\beta e^{i\omega_n\tau}G^{M}_{\alpha\beta}(\tau)d\tau\\
&= -\frac{1}{Z}\sum_{A,B}\langle A|\hat{\psi}_\alpha|B\rangle\,\langle B|\hat{\psi}^\dagger_\beta|A\rangle\,e^{-\beta E'_A}\int_0^\beta e^{i\omega_n\tau+(E'_A-E'_B)\tau}d\tau\\
&= -\frac{1}{Z}\sum_{A,B}\langle A|\hat{\psi}_\alpha|B\rangle\,\langle B|\hat{\psi}^\dagger_\beta|A\rangle\,\frac{1-\zeta_\psi e^{\beta(E'_A-E'_B)}}{i\omega_n+E'_A-E'_B}e^{-\beta E'_A}.
\end{aligned}$$

This also demonstrates the Eq. (2.25) :

$$G^{M}_{\alpha\beta}(i\omega_n)=\int_{-\infty}^{+\infty}d\varepsilon\frac{\rho_{\alpha\beta}(\varepsilon)}{i\omega_n-\varepsilon}.$$

The other Green function follow accordingly.

Let us provide a more physical interpretation to this retarded Green function at $T = 0$. For $t > 0$, we can always write $G^R_{\alpha\alpha}(t)$ as

$$G^R_{\alpha\alpha}(t) = -\langle GS|e^{i\hat{H}t}\hat{c}_\alpha e^{-i\hat{H}t}\hat{c}^\dagger_\alpha|GS\rangle - \langle GS|\hat{c}^\dagger_\alpha e^{i\hat{H}t}\hat{c}_\alpha e^{-i\hat{H}t}|GS\rangle\,.$$

Let us the initial electronic state as $|\psi_e(0)\rangle = \hat{c}^\dagger_\alpha|GS\rangle$ and its time-evolution as $|\psi_e(t)\rangle = e^{-i\hat{H}t}|\psi_e(0)\rangle$. We can have an equivalent writing for holes as $|\psi_h(0)\rangle = \hat{c}_\alpha|GS\rangle$. The Green function thus reads

$$G^R_{\alpha\alpha}(t) = -e^{iE_{GS}t}\langle\psi_e(0)|\psi_e(t)\rangle - e^{-iE_{GS}t}\langle\psi_h(t)|\psi_h(0)\rangle \text{ for t} > 0.$$

The retarded Green function thus measures the overlap between the electron and hole excitations at time $t = 0$ and time $t$ when they evolve under the action of the hamiltonian. If this states are eigenstates of $H$, then this is just phases. In general, they are not eigenstates and the Green function it measures the spreading of the electron and hole excitations.

### 2.4.2 Hilbert transform

We introduce the **Hilbert transform** of $\rho$ as

$$\mathcal{H}[\rho]_{ab}(z) = \int_{-\infty}^{+\infty} d\varepsilon \frac{\rho^{ab}(\varepsilon)}{z-\varepsilon},\ z \in \mathbb{C}\backslash\mathbb{R}. \tag{2.30}$$

One of the properties of this transformation is that

$$\mathcal{H}[\rho](\bar{z}) = (\mathcal{H}[\rho](z))^\dagger. \tag{2.31}$$

Utilizing this transform, the retarded and Matsubara Green functions can be simply written as

$$\begin{aligned} G^R(\omega) &= \mathcal{H}[\rho](\omega + i0^+) \\ G^M(i\omega_n) &= \mathcal{H}[\rho](i\omega_n). \end{aligned}$$

This is then clear that these two Green functions can be obtained using the analytical continuation $i\omega_n \to \omega + i0^+$.

Such analytical continuation is *a priori* far from obvious. Consider for example $f(z) = \sinh z\beta$, where $z = \frac{(2n+1)\pi}{\beta}$. The analytical continuation of this function gives $f(i\omega_n) = \sin((2n+1)\pi) = 0$, and thus $f = 0$ for all Matsubara frequencies. This prevents us from going backward and thus to recover the starting Green function by simply substituting $i\omega_n \to \omega + i0^+$. However, for Green functions, we know that they behave in the limit $\omega \to +\infty$ as $\frac{1}{z}$, which garantees the possibility to find such analytical continuation. Indeed, in the case where both $f(z)$ and $g(z)$ are equal for the Matsubara frequencies and behave as $\frac{1}{z}$ in the $z \to \infty$ limit, we know that $f = g$ and the correspondance is univocal.

In most problems, the calculations of the Green fucntions has to be done numerically and there are systematic errors in the calculations of Green functions. In the expression

$$G(\tau) = -\int d\varepsilon \rho(\varepsilon)\frac{e^{-\varepsilon\tau}}{1+e^{-\beta\varepsilon}},\ 0 \le \tau \le \beta,$$

the term $\frac{e^{-\varepsilon\tau}}{1+e^{-\beta\varepsilon}}$ is very small at large energy far from the Fermi level. The problem is then ill-posed. Indeed, the the Green function can be written as

$$G(\tau) = \sum_\varepsilon K(\varepsilon,\tau)\rho(\varepsilon),$$

where the term in $K(\varepsilon,\tau)$ is extremely small at high energy and typically within the systematic error bars. This makes the numerical analytical continuation rather tricky.

### 2.4.3 Sum over Matsubara frequencies

In many cases, we need to calculate a sum over Matsubara frequencies of the type $\frac{1}{\beta}\sum_n \phi(i\omega_n)$.

We typically assume that the function $\Phi(z)$ is meromorphic in the complex plane (i.e. only has a finite number of poles and no branch cuts). In most cases, the function $\Phi(z)$ will be a fraction.

Let us extend the Fermi (or simlarly the bose function) in the complex plane as $f(z) = \frac{1}{1+e^{\beta z}}$. The poles of $f$ are in $e^{\beta z} = -1$ and therefore in $z = i\omega_n$. The residue of $f$ in $z = i\omega_n$ is $-1/\beta$.

We now consider a circle $C$ parametrized by $z = Re^{i\theta}$ with $R \to \infty$. We use the fact that the integral $I$ on the contour $C$ satisfies

$$I = \oint_C f(z)\phi(z) = 0,$$

when taking $R \to \infty$. We can also apply the residue theorem to evaluate $I$ as

$$I = \sum_n (\frac{-1}{\beta})\phi(i\omega_n) + \sum_l f(z_l) Res(\phi, z_l),$$

where the sum over $l$ is the sum over all poles $z_l$ of the function $\phi$ and $Res(\phi, z_l)$ are the corresponding residues. We thus obtain the important result

$$\boxed{\frac{1}{\beta}\sum_n \phi(i\omega_n) = \sum_l f_D(z_l) Res(\phi, z_l)} \text{ for fermions.} \tag{2.32}$$

Therefore the Matsubara summation reduces to a summation over a finite (generally small) number of terms easily to calculate.

Had we consider bosonic Matsubara frequencies, we would obtain

$$\boxed{\frac{1}{\beta}\sum_n \phi(i\omega_n) = -\sum_l n_B(z_l) Res(\phi, z_l)} \text{ for bosons,} \tag{2.33}$$

where $n_B(z) = \frac{1}{e^{\beta z}-1}$.

## 2.5 2-particle correlation function

To be written.

# Chapitre 3

# Feynman diagrams

## 3.1 Notations

In what follows, we will study Hamiltonians of the follwoing form

$$\hat{H} = \hat{H}_0 + \hat{V},$$

where $\hat{H}_0$ is quadratic (and therefore integrable)

$$\hat{H}_0 = \sum M_{ab} \hat{c}_a^\dagger \hat{c}_b,$$

while $\hat{V}$ is a quartic interaction

$$\hat{V} = \frac{1}{2} \sum_{\lambda\mu\nu\rho} V_{\lambda\rho;\mu\nu} \hat{c}_\lambda^\dagger \hat{c}_\mu^\dagger \hat{c}_\nu \hat{c}_\rho.$$

The matrix element $V_{\lambda\rho;\mu\nu}$ verifies

$$V_{\lambda\rho;\mu\nu} = V_{\mu\nu;\lambda\rho}.$$

Since we can not calculate the single-particle Green functions for such a problem exactly, our goal will be to calculate them in perturbation theory. We wish to determine $G^M(\tau, \tau')$ in powers of $\hat{V}$. Our strategy will be composed of three parts

- Express $G^M$ of the interacting problem as series in $\hat{V}$ in order to obtain the correction to the $n^{\text{th}}$ order of the bare Green function noted $G_0^{(n)}$. We will use the interaction representation which is well suited here.
- Using the Wick theorem, we will see how to compute these Green functions $G_0^{(n)}$. The Wick theorem relies on $\hat{H}_0$ being quadratic (i.e. describes free particles).
- Finally we will calculate each term in the expansion in $\hat{V}$ using Feynman diagrams. This is the hardest part since it involves complicated integrals of order $n$ which may suffer from divergences.

## 3.2 Interaction representation

While the Heisenberg representation use the time-evolution of the full Hamiltonian $\hat{H}'$, the interaction representation only utilizes only the free Hamiltonian $\hat{H}'_0$. In this representation the time-evolution of an operator $\hat{A}$ is given by

$$\tilde{A}(\tau) = e^{\tau \hat{H}'_0} \hat{A} e^{-\tau \hat{H}'_0}. \tag{3.1}$$

We will try to keep the subscript $\tilde{A}$ to indicate the interaction representation. The expectation value of an observable $A$ is still given by

$$\langle A \rangle = \frac{1}{Z} \text{Tr}(e^{-\beta \hat{H}'} \hat{A}), \tag{3.2}$$

and we will define the free expectation value

$$\langle A \rangle_0 = \frac{1}{Z} \frac{\text{Tr}(e^{-\beta \hat{H}'_0} \hat{A})}{\text{Tr}(e^{-\beta \hat{H}'_0})} \tag{3.3}$$

Let us consider the Matsubara Green function $G^M_{ab}(\tau-\tau') = -\langle T_\tau \hat{c}_a(\tau)\hat{c}^\dagger_b(\tau')\rangle$, and the 2-body correlation function $\chi_{\alpha\beta\gamma\delta}(\tau_1,\tau_2,\tau_3,\tau_4) \equiv -\langle T_\tau(\hat{c}_\alpha(\tau_1)\hat{c}_\beta(\tau_1)\hat{c}^\dagger_\gamma(\tau_3)\hat{c}^\dagger_\delta(\tau_4))\rangle$.

For the former Green function, we will show that

$$\boxed{G^M_{ab}(\tau-\tau') = -\frac{\langle T_\tau \tilde{c}_a(\tau)\tilde{c}^\dagger_b(\tau')\exp\left(-\int_0^\beta du\tilde{V}(u)\right)\rangle_0}{\langle T_\tau \exp\left(-\int_0^\beta du\tilde{V}(u)\right)\rangle_0}}, \tag{3.4}$$

while the latter correlation is given by

$$\boxed{\chi_{\alpha\beta\gamma\delta}(\tau_1,\tau_2,\tau_3,\tau_4) = -\frac{\langle T_\tau \tilde{c}_\alpha(\tau_1)\tilde{c}_\beta(\tau_2)\tilde{c}^\dagger_\gamma(\tau_3)\tilde{c}^\dagger_\delta(\tau_4)\exp\left(-\int_0^\beta du\tilde{V}(u)\right)\rangle_0}{\langle T_\tau \exp\left(-\int_0^\beta du\tilde{V}(u)\right)\rangle_0}}. \tag{3.5}$$

Proof : We use the decomposition :

$$\hat{A}(\tau) = \hat{U}^{-1}(\tau)\tilde{A}(\tau)\hat{U}(\tau).$$

where we introduced the evolution operator $\hat{U}(\tau)$ defined by

$$\hat{U}(\tau) = e^{\tau\hat{H}'_0}e^{-\tau\hat{H}'}.$$

We wish to express the evolution operator in a simpler form. Let us take the derivative of it to obtain

$$\begin{aligned}\frac{d\hat{U}(\tau)}{d\tau} &= \hat{H}'_0 e^{\tau\hat{H}'_0}e^{-\tau\hat{H}'} + e^{\tau\hat{H}'_0}e^{-\tau\hat{H}'}(-\hat{H}') \\ &= e^{\tau\hat{H}'_0}(\hat{H}'_0-\hat{H}')e^{-\tau\hat{H}'} \\ &= -e^{\tau\hat{H}'_0}\hat{V}e^{-\tau\hat{H}'_0}e^{\tau\hat{H}'_0}e^{-\tau\hat{H}'}.\end{aligned}$$

And finally, we get

$$\frac{d\hat{U}(\tau)}{d\tau}(\tau) = -\tilde{V}(\tau)\hat{U}(\tau), \tag{3.6}$$

with the initial condition $\hat{U}(\tau=0)=\hat{1}$. The evolution operator can thus be expressed in terms of $\tilde{V}$ as

$$\hat{U}(\tau) = T_\tau\left(\exp\left(-\int_0^\tau du\tilde{V}(u)\right)\right). \tag{3.7}$$

We have included the time-ordering operator $T_\tau$. Its presence is actually necessary and makes sense if we expand the exponential in series. In this case, a typical term of the expansion reads $\int\int\int\cdots\int d\tau_1 d\tau_2 d\tau_3\cdots d\tau_n \tilde{V}(\tau_1)\tilde{V}(\tau_2)\tilde{V}(\tau_3)\cdots\tilde{V}(\tau_n)$, and the time ordering applies to all different terms in powers of $\tilde{V}$. In order to check that Eq. (3.7) satisfies to Eq. (3.6), let us take the derivative with respect to $\tau$. We thus obtain

$$\begin{aligned}\frac{d}{d\tau}T_\tau\left(\exp\left(-\int_0^\tau du\tilde{V}(u)\right)\right) &= T_\tau\left[-\tilde{V}(\tau)\exp\left(-\int_0^\tau \tilde{V}(u)du\right)\right] \\ &= -\tilde{V}(\tau)\hat{U}(\tau),\end{aligned}$$

and we indeed recover the form in Eq. (3.7).

Let us now show the expression in Eq. (3.4) of the Matsubara Green function. The partition function reads

$$\begin{aligned}Z = \mathrm{Tr}(e^{-\beta\hat{H}'}) &= \mathrm{Tr}\left(e^{-\beta\hat{H}'_0}e^{\beta\hat{H}'_0}e^{-\beta\hat{H}'}\right) \\ &= \mathrm{Tr}\left(e^{-\beta\hat{H}'_0}T_\tau\exp\left(-\int_0^\beta \tilde{V}(u)du\right)\right) \\ &= Z_0\left\langle T_\tau\exp\left(-\int_0^\beta \tilde{V}(u)du\right)\right\rangle_0.\end{aligned}$$

Let us introduce $\hat{S}(\tau,\tau') = \hat{U}(\tau)\hat{U}^{-1}(\tau')$. We do have $\hat{S}(\tau,0) = \hat{U}(\tau)$. We also have $\hat{S}(\tau_1,\tau_2)\hat{S}(\tau_2,\tau_3) = \hat{S}(\tau_1,\tau_3)$ This is to show that

$$\hat{S}(\tau,\tau') = T_\tau e^{-\int_{\tau'}^{\tau}\tilde{V}(u)du}.$$

We want to calclulate the 2-point correlation function. Let us focus on the numerator and assume $\tau > \tau'$.

$$\begin{aligned}(\hat{c}_a(\tau)\hat{c}_b^\dagger(\tau')) &= \mathrm{Tr}\left(T_\tau(e^{-\beta\hat{H}_0'}\hat{U}^{-1}(\tau)\tilde{c}_a(\tau)\hat{U}(\tau)\hat{U}^{-1}(\tau')\tilde{c}_b^\dagger(\tau')\hat{U}(\tau'))\right)\\ &= \mathrm{Tr}\left(e^{-\beta\hat{H}_0'}\hat{S}(\beta,0)\hat{S}(0,\tau)\tilde{c}_a(\tau)\hat{S}(\tau,0)\hat{S}(0,\tau')\tilde{c}_b(\tau')\hat{S}(\tau',0)\right)\\ &= \mathrm{Tr}\left(e^{-\beta\hat{H}_0'}\hat{S}(\beta,\tau)\tilde{c}_a(\tau)\hat{S}(\tau,\tau')\tilde{c}_b(\tau')\hat{S}(\tau',0)\right)\\ &= \mathrm{Tr}\left(T_\tau e^{-\beta\hat{H}_0'}\tilde{c}_a(\tau)\tilde{c}_b(\tau')\hat{S}(\beta,0)\right).\end{aligned}$$

In order to go from the 3rd to the 4th line, we use the fact that $0 < \tau' < \tau < \beta$, therefore the operators in the 3rd line were already time-ordered. We could therefore reshuffle all the operators under the time-ordering sign to simplify the expression. Notice that since $V$ is quartic in the number of operators, there is no sign coming in.

Combining these two results, we indeed find Eq. (3.4). We can do exactly the same reasoning had we assumed $\tau < \tau'$. A similar reasoning also allows to demonstrate the Eq. (3.5). Notice that these results are general and rely and the interaction representation. $H_0$ does not need to be quadratic at this stage. We only assume thermal equilibrium (i.e. imaginary-time translation invariance).

## 3.3 Some technical remarks

In what follows, we will need to calculate the sum of a function over Matsubara frequencies like

$$\frac{1}{\beta}\sum_n \phi(i\omega_n),$$

where $\phi$ is some regular function in $\mathbb{C}$. To do so, we introduce the Fermi function $n_F(z)$ extended in the complex plane :

$$n_F(z) = \frac{1}{1+e^{\beta z}}.$$

The poles of $n_F(z)$ are located in $z = i\omega_n$, where $\omega_n$ are the fermionic Matsubara frequencies (for fermions, $\omega_n = \pi T(2n+1)$). Let us integrate the function $\phi(z)$ multiplied by the Fermi Dirac function in the whole complex plane along a circular contour $\mathcal{C}$ centered around the origin $O$ and of radius $R \to \infty$. We therefore obtain

$$\int_{\mathcal{C}} \frac{dz}{2i\pi} n_F(z)\phi(z) = -\frac{1}{\beta}\sum_n \phi(i\omega_n) + \sum_l r_l n_F(z_l) = 0,$$

where $z_l$ are the poles of the function $\phi$ with residues $r_l$ (notice that the residues of $n_F(z)$ in $z = i\omega_n$ are given by $-\frac{1}{\beta}$). The function $n_F(z)\phi(z)$ being regular in $\mathbb{C}$, the whole integral should be 0. We thus obtain the following result :

$$\frac{1}{\beta}\sum_n \phi(i\omega_n) = \sum_l r_l n_F(z_l). \tag{3.8}$$

To illustrate this result, let us consider the following simple example :

$$\phi(i\omega_n) = \frac{e^{i\omega_n 0^+}}{i\omega_n - \varepsilon}.$$

That function has a single pole $z_l = \varepsilon$ de résidu 1. We can therefore infer using Eq. (3.8) that

$$\frac{1}{\beta}\sum_n \frac{e^{i\omega_n 0^+}}{i\omega_n - \varepsilon} = n_F(\varepsilon).$$

## 3.4 Wick Theorem

### 3.4.1 The theorem

**Theorem 1** *We consider a quadratic Hamiltonian given by*

$$\hat{H}_0 = \sum_{\alpha,\beta} \hat{c}_\alpha^\dagger M_{\alpha\beta}\hat{c}_\beta.$$

*In the case of fermions, the 2n-particles correlation functions can be written using the Wick theorem as follows :*

$$\langle T_\tau \hat{c}_{\alpha_1}(\tau_1)\cdots\hat{c}_{\alpha_n}(\tau_n)\hat{c}^\dagger_{\alpha'_n}(\tau'_n)\cdots\hat{c}^\dagger_{\alpha'_1}(\tau'_1)\rangle_0 = \sum_{P\in\mathbb{S}_n} sgn(P)\prod_{k=1}^{n}\langle T_\tau \hat{c}_{\alpha_k}(\tau_k)\hat{c}^\dagger_{\alpha'_{P_k}}(\tau'_{P_k})\rangle_0, \tag{3.9}$$

where $\mathrm{sgn}(P)=\zeta_P=(-1)^{\text{number of exchanges}}$. Actually, if we set $\hat{A}_\alpha=\hat{c}_\alpha$ or $\hat{c}^\dagger_\alpha$, a slighly more general form of the Wick theorem states that

$$\langle T_\tau \hat{A}_1(\tau_1)\cdots\hat{A}_{2n}(\tau_{2n})\rangle = \sum_{\mathcal{P}}\zeta_P\prod_{k=1}^{n}\langle T_\tau \hat{A}_{i_k}(\tau_{i_k})\hat{A}_{j_k}(\tau_{j_k})\rangle.$$

For bosons, we do have $\zeta_P=1$.

The conditions of applications of the Wick theorem are that $H_0$ shall be quadratic and the operators $\hat{A}_\alpha$ obey canonical commutations relations (i.e. commutation or anticommutation relations).

Therefore, there is no Wick theorem for spin operators !

### 3.4.2 Its Proof

This is quite cumbersome and not so useful. I will recommend instead the one given in Bruus and Flensberg p 199 for those who are interested.

### 3.4.3 Use of the theorem

This is obviously more important than its proof for practical use. Let us consider the ordered product of 4 creation and destruction operators according to

$$T_\tau \tilde{c}_{\alpha_1}(\tau_1)\tilde{c}_{\alpha_2}(\tau_2)\tilde{c}^\dagger_{\beta_1}(\tau_3)\tilde{c}^\dagger_{\beta_2}(\tau_4),$$

and let us calculate its average. The Wick theorem told us that this expresion can be decomposed in products of quadratic averages. We see that the terms $\tilde{c}\tilde{c}$ where $\tilde{c}^\dagger\tilde{c}^\dagger$ give a zero contribution. Therefore the only two non-zero contributions are the terms $(1,3)$ and $(2,4)$ for the first case and $(1,4)$ and $(2,3)$ for the second one. The first term (A)has a $-$ sign due to the permutation of the operators to pair them while the second term (B) has a $+$ sign. We finally obtain

$$\begin{aligned}\langle T_\tau \tilde{c}_{\alpha_1}(\tau_1)\tilde{c}_{\alpha_2}(\tau_2)\tilde{c}^\dagger_{\beta_1}(\tau_3)\tilde{c}^\dagger_{\beta_2}(\tau_4)\rangle_0 \;=\; & -\langle T_\tau \tilde{c}_{\alpha_1}(\tau_1)\tilde{c}^\dagger_{\beta_1}(\tau_3)\rangle_0\langle T_\tau \tilde{c}_{\alpha_2}(\tau_2)\tilde{c}^\dagger_{\beta_2}(\tau_4)\rangle_0 \\ & +\langle T_\tau \tilde{c}_{\alpha_1}(\tau_1)\tilde{c}^\dagger_{\beta_2}(\tau_4)\rangle_0\langle T_\tau \tilde{c}_{\alpha_2}(\tau_2)\tilde{c}^\dagger_{\beta_1}(\tau_3)\rangle_0 .\end{aligned}$$

## 3.5 Perturbative expansion of the Green functions and Feynman diagrams

The idea behind the perturbative expansion consists in expanding the term $\exp\left[-\int_0^\beta du\tilde{V}(u)\right]$ in powers of $\tilde{V}(u)$ as $1-\int_0^\beta \tilde{V}(u)du+\frac{1}{2}\int_0^\beta\int_0^\beta \tilde{V}(u_1))\tilde{V}(u_2)du_1du_2+\cdots$ and then use the Wick theorem to decompose the average values containing several operators as products of the form $\langle T_\tau\tilde{c}_\alpha\tilde{c}^\dagger_\beta\rangle_0$ in both the numerator and the denominator At first order, this gives for $G_{\alpha\beta}(\tau-\tau')$

$$G_{\alpha\beta}(\tau-\tau') = -\langle T_\tau\tilde{c}_\alpha(\tau)\tilde{c}^\dagger_\beta(\tau')\rangle_0 + \int_0^\beta du\,\langle T_\tau\tilde{c}_\alpha(\tau)\tilde{c}^\dagger_\beta(\tau')\tilde{V}(u)\rangle_0 + \int_0^\beta du\,\langle T_\tau\tilde{c}_\alpha(\tau)\tilde{c}^\dagger_\beta(\tau')\rangle_0\langle\tilde{V}(u)\rangle_0$$

At first order, our Green function can be written as the sum of two terms

$$G = G^0 + G^1,$$

where $G^0$ is the non-interacting Green function and $G^1$ is the first order of the perturbation theory which can be written formally as

$$G^1 = \int_0^\beta du\frac{1}{2}\sum_{\lambda\rho,\mu\nu}V_{\lambda\rho,\mu\nu}K,$$

where $K$ is given as

$$K = \langle T_\tau \tilde{c}_\alpha(\tau)\tilde{c}^\dagger_\beta(\tau')\tilde{c}^\dagger_\lambda(u)\tilde{c}^\dagger_\mu(u)\tilde{c}_\nu(u)\tilde{c}_\rho(u)\rangle_0 - \langle T_\tau \tilde{c}_\alpha(\tau)\tilde{c}^\dagger_\beta(\tau')\rangle_0 \langle T_\tau \tilde{c}^\dagger_\lambda(u)\tilde{c}^\dagger_\mu(u)\tilde{c}_\nu(u)\tilde{c}_\rho(u)\rangle_0 .$$

The first term (A) given by the Wick theorem is obtained by contracting the $\alpha$ and $\beta$ operators in both terms in $K$. However, these two terms cancel each other exactly. The next possible contractions are on one hand $B = (\alpha,\lambda),(\beta,\nu),(\mu,\rho)$ and $C = (\alpha,\mu),(\beta,\rho),(\lambda,\nu)$. However due to the symmetry of $V_{\lambda\rho;\mu\nu} = V_{\mu\nu;\lambda\rho}$ we do have $B = C$. These two terms are called Fock terms and appear with a global $-$ sign. Finally the last two contributions are $E = (\alpha,\mu),(\beta,\nu),(\lambda,\rho)$ and $D = (\alpha,\lambda),(\beta,\rho),(\mu,\nu)$. Once again these two terms are equal to each other and thus $E = D$. This rerm appears with a global + sign. The two non-zero terms (actually 2*2 in total)are products of three bare Green functions. We obtain for $G^1_{\alpha\beta}$ the following expression

$$G^1_{\alpha\beta}(\tau-\tau') = \sum_{\mu\nu,\rho\lambda}\int du V_{\lambda\rho,\mu\nu}\left[-G^0_{\alpha\lambda}(\tau-u)G^0_{\nu\beta}(u-\tau')G^0_{\rho\mu}(0^-) + G^0_{\alpha\lambda}(\tau-u)G^0_{\rho\beta}(u-\tau')G^0_{\nu\mu}(0^-)\right].$$

Let us simplify the previous expression. Let us consider in that purpose the integral of $A(\tau-u)B(u-\tau')$. By expanding over the Matsubara frequencies, we obtain

$$\int_0^\beta du A(\tau-u)B(u-\tau') = \frac{1}{\beta^2}\sum_{n_1,n_2}\int_0^\beta du A(i\omega_{n_1})B(i\omega_{n_2})e^{-i\omega_{n_1}(\tau-u)}e^{-i\omega_{n_2}(u-\tau')}.$$

As $\int_0^\beta du e^{iu(\omega_{n_1}-\omega_{n_2})} = \beta\delta_{n_1,n_2}$, we can simplify the integral over $u$ and obtain

$$\frac{1}{\beta}\sum_n A(i\omega_n)B(i\omega_n)e^{-i\omega_n(\tau-\tau')} = FT(A(i\omega_n)B(i\omega_n)).$$

Finally in Fourier space, we find that the expression of $G^1_{\alpha\beta}$ is given by

$$G^1_{\alpha\beta}(i\omega_n) = \sum_{\lambda\rho,\mu\nu} V_{\lambda\rho,\mu\nu}\left[G^0_{\alpha\lambda}(i\omega_n)G^0_{\beta\rho}(i\omega_n)\langle\tilde{c}^\dagger_\mu\tilde{c}_\nu\rangle_0 - G^0_{\alpha\lambda}(i\omega_n)G^0_{\nu\beta}(i\omega_n)\langle\tilde{c}^\dagger_\mu\tilde{c}_\rho\rangle_0\right].$$

This is the final result. The method we used appears quite cumbersome already at first order. Needless that such method is likely to be filled with mistakes at higher order. The diagrammatic approach is actually an alternative approach and enables a direct calculation of $G^{(n)}_{\alpha\beta}$ from diagrams built according to **Feynman rules**. These diagrams use two types of objects :

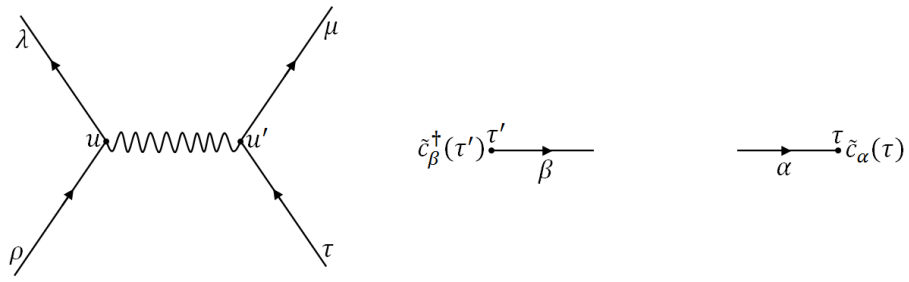


(a) (b)

FIGURE 3.1 – (a) Vertex and (b) external legs of the Feynman diagrams

i) The vertex diagrams (see FIGURE(3.1.a)). These vertex are related to the interaction

$$-V_{\lambda\rho;\mu\nu}\delta(u-u')\tilde{c}^\dagger_\lambda(u)\tilde{c}^\dagger_\mu(u')\tilde{c}_\nu(u')\tilde{c}_\rho(u). \tag{3.10}$$

This part of the diagrams possesses an inversion symmetry due to the invariance of $V$ when exchanging $\lambda\rho$ and $\mu\nu$. The diagrams are also composed of two external legs (see FIGURE(3.1.b)). These two legs correspond to the

two creation and annihilation operators respectively $\tilde{c}^\dagger_\beta(\tau')$ and $\tilde{c}_\alpha(\tau)$. The diagrams are then formed by connecting these external legs to the vertex. The number of vertex is equal to the degree of expansion in $V$ of the Green function. In the figure, we have used two different labels for the variables $u$ and $u'$. This corresponds a priori to the time-delay of the Coulomb interaction (no interaction is instantaneous). However, this time is extremely fast compared to the time scale we are interested in. Therefore, we can fairly assume $u = u'$ as we did in Eq. (3.10) with the delta distribution.

At first order in $V$, the possible diagrams which can be drawn from one vertex and two external legs are depicted in Fig. (3.2). The first of this term in Fig. (3.2.a) is equivalent to the (A) contribution. This diagam is however non-connected. A general property of the Feynman diagrams is that the non-connected diagrams bring a zero contribution to the Green function (we won't show this property but the reader can convince himself going back to the definition of Green function). In what follows we will not draw these disconnected diagrams.

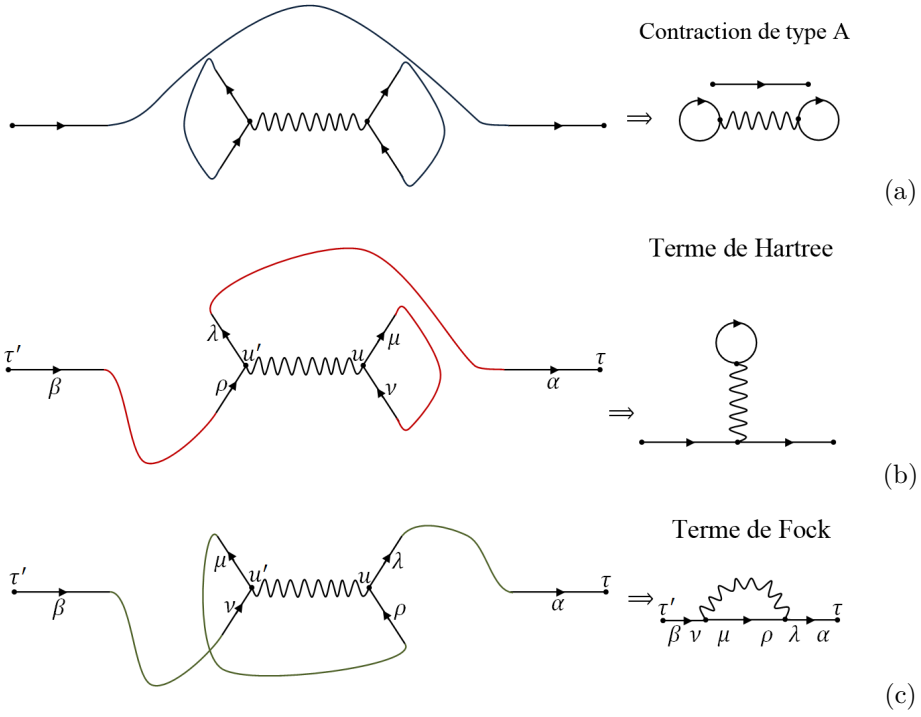


FIGURE 3.2 – Contribution of order (1) to the Matsubara Green function : (a) Term of type (A) (b) Hartree diagram (c) Fock diagram. The right figures correspond simply to the condensed drawing of the figures in the left.

ii) The second contribution in (3.2.b) is formed from a line of particles and a loop linked by a propagator. This term is equivalent to the previous Hartree term. The calculation of the Green function is as follows : we associate every line of the diagram to a bare Green function $G^0_{\psi\xi}$ where the two indices $\psi\xi$ belong to two different legs of the diagram connected to each other taken in the order opposite to the direction of the arrow. The time variables of the Green functions follow a similar rule. We therefore obtain for this diagram the following contribution

$$G^0_{\rho\beta}(u-\tau')G^0_{\alpha\lambda}(\tau-u)G_{\nu\mu}(0^-),$$

where we assumed $u = u'$. The global sign in front of this term will be detailed further. We will need to integrate over $u$. Notice that with have a single loop which is related to the order of the expansion.

Finally, the last contribution to the Green function is the term in Fig. (3.2.c). This term corresponds to the Fock term previously discussed. It is built from a line (representing a bare Green function) from which a propagator is emitted and then reabsorbed to give another line. As for the Hartree term, there is a single loop and therefore a single integration over $u$ too. Following our prescription, the contribution to the Green function of this diagram

$$-G^0_{\nu\beta}(u-\tau')G^0_{\rho\mu}(0^-)G^0_{\alpha\lambda}(\tau-\mu),$$

where the global $-$ sign will be further explained. Notice that the indices of the vertex have been modified in this diagram compared to Fig. (3.2.b) following the symmetry of $V_{\lambda\rho,\mu\nu}$.

From this three diagrams, we have built a representation of $G^1$. It is even (far) easier to obtain it frequency space since less indices are involved. Indeed, we must ensure conservation of the frequency (energy) at every nodes of the diagram and sum over all intermediate frequencies. Therefore, for the Hartree diagram in Fig. (3.2.b), we have for the Green function in frequency space :

$$G^{1-\text{Hartree}}_{\alpha\beta}(i\omega_n) = G^0_{\alpha\lambda}(i\omega_n)G^0_{\rho\beta}(i\omega_n)\sum_{n_1} G^0_{\nu\mu}(i\omega_{n_1})e^{i\omega_{n_1}0^+},$$

where the term $e^{i\omega_{n_1}0^+}$ is just added to ensure the convergence of the whole Green function.

## 3.6 Feynman rules

In order to build the Feynman diagrams, we can enumerate the following 7 general rules. For a term of order $n$ in $V$,

1. Draw all topologically distinct diagrams with two external legs and $n$ vertices
2. The frequency should be conserved at all nodes of the diagrams.
3. Every vertex should be taken with a factor $V_{\lambda\rho,\mu\nu}\delta(u-u')$.
4. To every line, we associate the propagator $G^0_{\alpha\beta}(i\omega_n)$.
5. We sum over all internal degrees of freedom $(\lambda,\alpha,\beta,\rho,\cdots)$ and all internal frequencies.
6. We associate a sign $(-1)^n(-1)^F$ to every diagram where $n$ is the order of the expansion and $F$ the number of **fermionic** loops.
7. Ensure the conservation of momentum for each vertex.

The sixth rule give us access to the global signs in front of each diagram in the calculation of the Green function. We therefore see that for the diagram in Fig. (3.2.b), the expansion corresponds to $n=1$, and the diagram contains one fermionic loop so $F=1$. We therefore obtain a whole contribution $+1$ and a global $+$ sign. Concerning the Fock diagram depicted in Fig. (3.2.c), we find a global $-$ sign due to the absence of fermionic loop.

To illustrate these rules, let us consider the Hamiltonian $\hat{H}_0 = \sum_{k,\sigma}\varepsilon_k\hat{c}^\dagger_{k,\sigma}\hat{c}_{k,\sigma}$, with the perturbation

$$\hat{V} = \frac{1}{\mathcal{V}}\sum_{k_1,k_2,q}\left[\frac{1}{2}V_\parallel(q)\sum_{\sigma=\uparrow,\downarrow}\hat{c}^\dagger_{k_1+q,\sigma}\hat{c}^\dagger_{k_2-q,\sigma}\hat{c}_{k_2,\sigma}\hat{c}_{k_1,\sigma} + \frac{1}{2}V_A(q)\hat{c}^\dagger_{k_1+q,\uparrow}\hat{c}^\dagger_{k_2-q,\downarrow}\hat{c}_{k_2,\downarrow}\hat{c}_{k_1,\uparrow}\right],$$

where $\mathcal{V}$ denotes the volume. Moreover, we assume inversion symmetry, nnamely $V_\parallel(-q) = V_\parallel(q)$.

The vertices associated with these perturbations are represented in Figs (3.3.a) and (3.3.b) for $V_\parallel$ and $V_A$ respectively.

The explicit form of $V_\parallel$ and $V_A$ depends on the type of interaction $V(r)$ used. For example, for the Coulomb interaction $V(r) = \frac{e^2}{4\pi\varepsilon_0}\frac{1}{|r|}$, we obviously obtain that $V_A(q) = V_\parallel(q) = \frac{e^2}{\varepsilon_0 q^2}$, while for a local interaction such as $V(r) = g\delta(r)$ where $g$ denotes a constant (typically $= \frac{4\pi\hbar^2 a}{m}$ for cold atoms), $V_\parallel = 0$ whereas $V_a(q) = g$.

With this general form where $V_\parallel$ and $V_A$ are not specified, the Hartree term reads (using momentum conservation) :

$$\begin{aligned} G^1_{k\uparrow}(i\omega_n) &= G^0_k(i\omega_n)G^0_k(i\omega_n)\sum_{n'}\int\frac{d^3k'}{(2\pi)^3}\frac{1}{\beta}G^0_{k'}(i\omega_{n'})e^{i\omega_n 0^+}V(q=0) \\ &= \frac{1}{(i\omega_n-\varepsilon_k)^2}\left[V_\parallel(q=0)\langle n_\uparrow\rangle_0 + \frac{1}{2}V_A(0)\langle n_\downarrow\rangle_0\right], \end{aligned}$$

where $\langle n_\uparrow\rangle_0$ is given by

$$\langle n_\uparrow\rangle_0 = \int\frac{d^3k}{(2\pi)^3}\langle\hat{c}^\dagger_{k\uparrow}\hat{c}_{k\uparrow}\rangle = \int\frac{d^3k}{(2\pi)^3}\frac{1}{\beta}\sum_{\omega_n}\frac{e^{i\omega_n 0^+}}{i\omega_n-\varepsilon_k}.$$

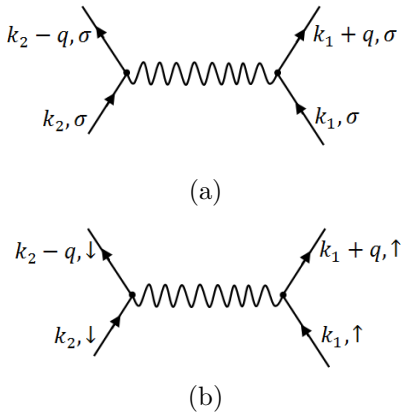


FIGURE 3.3 – (a) Vertex associated with $V_\parallel$ (b) Vertex associated with $V_A$.

Finally concerning the Fock term, we see that the $V_A$ term does not contribute due to spin conservation, and the contribution to the Green function is

$$G_k^1(i\omega_n) = -G_k^0(i\omega_n)G_k^0(i\omega_n)\frac{1}{\beta}\sum_{\omega_{n_1}}\sum_q G_{k+q}^0(i\omega_n + i\omega_{n_1})e^{i(\omega_n+\omega_{n_1})0^+}.$$

Using

$$\frac{1}{\beta}\sum_{\omega_{n_1}} G_{k+q}^0(i\omega_n + i\omega_{n_1}) = \frac{1}{\beta}\sum_{\omega_{n_1}} G_{k+q}^0(i\omega_{n_1})e^{i\omega_{n_1}0^+} = n_F(\varepsilon_{k+q}),$$

We obtain the Fock contribution to the Green function $G_{k\uparrow}^1$ is

$$G_{k\uparrow}^1(i\omega_n) = -\frac{1}{(i\omega_n - \varepsilon_k)^2}\sum_q V_\parallel(q)n_F(\varepsilon_{k+q})$$

We have seen that the Green functions can be rewritten as the sum of diagrams. Hence, at first order the previous problem can be summarized picturally as in Fig. 3.4.

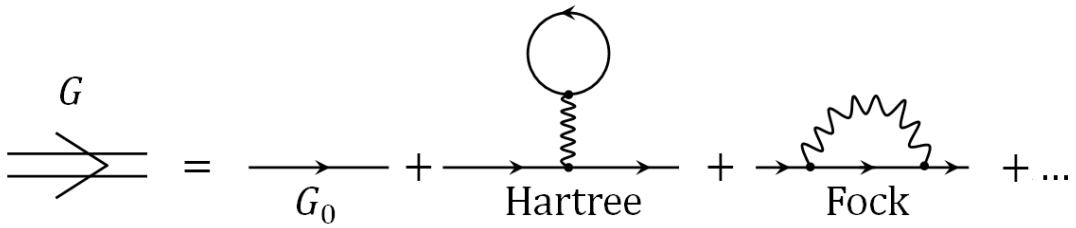


FIGURE 3.4 – Diagrammatic expansion of the interacting Green function at first order in perturbation theory

Let us see how the introduction of the *self-energy* allows to simplify the calculations and can improve the approximation by resuming certain types of diagrams. Let us define $\Sigma_H(k, i\omega_n)$, the self-energy of the Hartree term as

$$\Sigma_H(k, i\omega_n) = \quad = V_\parallel(0)\langle n_\uparrow\rangle_0 + V_A(0)\langle n_\downarrow\rangle_0 .$$

We can extract a class of diagrams that we can sum up. We therefore obtain the following geometric series :

$$+ \cdots = G_0\left[1 + \sum_{n=1}^{\infty}(\Sigma_H G_0)^n\right]$$

$$= \frac{1}{1 - \Sigma_H G_0} = \frac{1}{G_0^{-1} - \Sigma_H},$$

and finally, this sum of diagrams gives for $G_H$

$$G_H = \frac{1}{i\omega_n - (\varepsilon_k - \mu) - \Sigma_H}.$$

As we did for the Hartree term, it is possible to treat the Fock terms similarly as follows :

$$\Sigma_F = -\sum_q V_\parallel(q)n_F(\varepsilon_{k+q})$$

$$G_F = + + + + \cdots$$

More generally, it is possible to obtain the Green function by resuming combinations of diagrams as follows :

$$G_0 + G_0(\Sigma_H + \Sigma_F)G_0 + G_0(\Sigma_H + \Sigma_F)G_0(\Sigma_H + \Sigma_F)G_0 + \cdots = \frac{1}{i\omega_n - (\varepsilon_k - \mu) - (\Sigma_H + \Sigma_F)}$$

$$= \frac{\longrightarrow}{1 - \left( \circ + \text{wiggle} \right) \cdot \longrightarrow}$$

Therefore, we obtain

$$G(k, i\omega_n) = \frac{G_0(k, i\omega_n)}{1 - G_0(k, i\omega_n)\Sigma(k, i\omega_n)},$$

where the poles of the Green function $G$ will depend on the self-energy $\Sigma$ which is a regular function. This self-energy is the exact **irreducible** one which is composed of the sum of all the 2-leg diagrams which cannot be separated in two disjunct pieces by severing one propagator (this is what the term irreducible means).

At second order in perturbation theory, this self-energy contains the following terms :

$\Sigma =$ 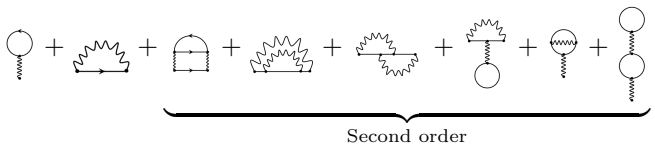 Second order

The first second order diagram for the self-energy is the bubble diagram which is quite important. We will compute it in the tutorial. The second one is the rainbow diagram. Calculating these diagrams is actually already difficult at second order as you will see. Therefore, at higher order, the number of diagrams will explode and their analytical calculation becomes problematic not to say hopless. Fortunately, not all of them are important. We clearly see that we will need to develop some numerical techniques to generate ansd especially evaluate them. Such method exists ans is called Diagrammatic Monte Carlo method.

**Example :** To illustrate these results, we consider a short-range interaction such that

$$V_A(q) = \frac{4\pi\hbar^2 a}{m}, \; V_\parallel(q) = 0.$$

The self-energy which takes into account both the Hartree and Fock terms (here the Fock term is zero)) reads

$$\Sigma_\sigma^{HF}(k, i\omega_n) = V_A(0) \langle n_{-\sigma} \rangle \in \mathbb{R}.$$

The self-energy is here real. This indicates that its main effect is to shift the chemical potential. No broadening is obtained at this order. We need to go to higher order in perturbation theory to find some imaginary part to the self-energy. Gathering all previous terms, we find

$$\Sigma_\sigma^{HF}(k, i\omega_n) = \frac{4\pi\hbar^2 a}{m} \frac{k_F^3}{6\pi^2}.$$

Introducing this expression back into our Green function, we finally obtain

$$G(k, i\omega_n) = \frac{1}{i\omega_n - \left(\frac{\hbar^2 k^2}{2m} - \mu\right) - \Sigma^{HF}}.$$

The self-energy being real, the poles of $G(k, i\omega_n)$ are obtained for $i\omega_n = 0$ which enables to define the chemical potential as a function of $k_F$ as

$$\mu - \varepsilon_{k_F} - \Sigma^{HF}(k_F, i\omega_n = 0) = 0. \tag{3.11}$$

This equation is actually general and define the Fermi surface in an interacting problem of fermions.

In our case (at $T = 0$), we do have therefore

$$\mu = \frac{\hbar^2 k_F^2}{2m} + \Sigma^H = \frac{\hbar^2 k_F^2}{2m} \left(1 + \frac{4}{3\pi} k_F a + \cdots\right). \tag{3.12}$$

For a Fermi liquid, whatever the interactions are, the following relation holds :

$$n = n_\downarrow + n_\uparrow = \frac{k_F^3}{3\pi^2}.$$

This is known as the Luttinger theorem and we will not demontrstate it. Notice that we already demonstrate it for non-interacting fermions in Chap. 1. The point is that it holds for interacting fermions provided the Fermi surface (momentum) is defined accordingly as in Eq. (3.11).

The chemical potential is defined as the derivative of the energy with respect to $N$ the number of particles. The ground state energy therefore reads

$$E_{GS} = \int_0^N dN' \mu(N').$$

Utilizing the following result

$$\int_0^N dN' k_F^\lambda = \frac{3}{3+\lambda} k_F^\lambda N,$$

we infer the energy per particle of a non-perfect Fermi gas :

$$\frac{E_{GS}}{N} = \frac{\hbar^2 k_F^2}{2m}\left(\frac{3}{5} + \frac{2}{3\pi} k_f a + \cdots\right). \tag{3.13}$$

Another way to compute the ground state energy per particle is possible using the partition function which can be written as a product of the non-interacting partition function times an interacting one :

$$Z = Z_0 \left\langle T_\tau e^{-\int_0^\beta du \tilde{V}(u)} \right\rangle \ .$$

We can thus deduce the free energy as

$$F = -\frac{1}{\beta} \ln Z = -\frac{1}{\beta} \ln Z_0 - \frac{1}{\beta} \ln \langle \left[ T_\tau e^{-\int_0^\beta du \tilde{V}(u)} \right] \rangle.$$

The first term simply provides the non-interacting free energy $F_0$ while the second can be calculated by a diagrammatic expansion which at first order is limited to the Hartree and Fock terms

$\delta F =$ 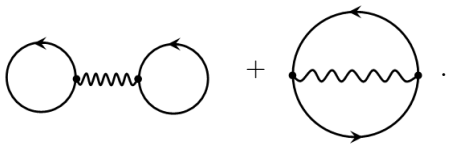 .

However, spin conservation at the vertex forbids the second Fock term and only the Hartree term $V_A(0) n_\downarrow n_\uparrow$ subsists. The first order contribution provides the energy per unit volume as

$$\frac{\delta F}{V} = V_A(0) n_\uparrow n_\downarrow = \frac{4\pi\hbar^2 a}{m} \frac{k_F^3}{6\pi^2} \frac{k_F^3}{6\pi^2} = \frac{4\pi\hbar^2 a}{m} \frac{N}{2V} \frac{k_F^3}{6\pi^2},$$

and finally, we also recover the first order contribution to the free energy as

$$\frac{\delta F}{N} = \frac{\hbar^2 k_F^2}{2m}\left(\frac{2}{3\pi} k_F a\right). \tag{3.14}$$

As a final remark, I would like to emphasize that we just scratch the surface and present first order diagrams. There techniques to resum some class of diagrams such as the RPA or the parquet resummation techniques which we will not discuss. We minaly focuss on the teh single-particle Green function and asscociated self-energy. However, we are interested in 2-particle correlation function, we need to take into account the renormalization of the vertex therefore of the interaction itself. This involves other class of diagrams with four legs.

## 3.7 Diagrammatic approach of the resonant level model

Let us apply the diagrammatic method to a problem we already solved. We thererfore reconsider the resonant level Hamiltonian

$$\hat{H} = \sum_k \varepsilon_k \hat{c}_k^\dagger \hat{c}_k + \varepsilon_d \hat{d}^\dagger \hat{d} + \frac{t}{\sqrt{V}} \sum_k \left( \hat{c}_k^\dagger \hat{d} + \text{h.c.} \right).$$

Exercice : Using a diagrammatic approach, calculate the Green function

$$G_d(\tau - \tau') = -\langle T_\tau \hat{d}(\tau) \hat{d}^\dagger(\tau') \rangle = -\frac{\langle T_\tau \tilde{d}(\tau) \tilde{d}(\tau') e^{-\int_0^\beta du \tilde{V}(u)} \rangle}{\langle T_\tau e^{-\int_0^\beta du \tilde{V}(u)} \rangle}.$$

The interaction couples a discrete level $|d\rangle$ to a continuum $|c\rangle$. The interaction Hamiltonian thus reads $\hat{H}_{int} = \frac{t}{\sqrt{V}} \sum_k \left( \hat{c}_k^\dagger \hat{d} + \text{h.c.} \right)$. Since the problem is quadratic, the diagrammatic apptroach is a priori is not really needed here. Our goal is only to illustrate it. The interaction being 2-body, the diagrams are only linear here. The $0^{\text{th}}$ order of the expansion is simply given by the bare propagator :

$$G_d^0(i\omega_n) = \frac{1}{i\omega_n - \varepsilon_d}.$$

The first order term implies a single vertex interaction $t/\sqrt{V}$, connecting the states $|c\rangle$ and $|d\rangle$. Because $\langle \hat{c}^\dagger \hat{d} \rangle_0 = 0$ (the bare Hamiltonian does not connect $|c\rangle$ and $|d\rangle$), the first order term is 0. Actually, from the Wick theorem, this is true for all terms contianing an odd number of $|c\rangle$ or $|d\rangle$ states. Therefore, only the contribution with an even number of vertex are non zero. In particular, the second order diagram is given by

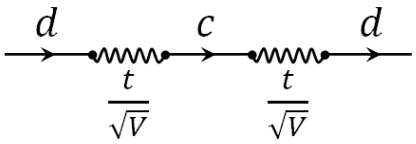


The contribution of this diagram to the Green function can be written as

$$G_d^{(2)} = G_d^0(i\omega_n) \frac{t}{\sqrt{V}} \sum_k G_k^0(i\omega_n) \frac{t}{\sqrt{V}} G_d^0(i\omega_n),$$

where $G_k^0(i\omega_n) = \frac{1}{i\omega_n - \varepsilon_k}$ is the bare Green function for the state $|k\rangle$ We need to sum over all momenta since momentum conservation implies that only the initial and final momenta to be the same (actually the impurity breaks translation invariance so we need to sum over all possible momenta). However, energy conservation implies that the Matsubara frequencies should be the conserved for all vertex. Therefore all intermediate Green function should be taken at the same pulsation $i\omega_n$.

We can continue the expansion for all even orders to obtain the contribution of order $2n$ denoted $G^n$ to simplify the notations

$$G_d^n = G_d^0 \left( \frac{t^2}{V} \right)^n \left( G_d^0 \sum_k G_c^0 \right)^n.$$

Suming these terms, we recover a geometric series and we finally can write

$$G_d(i\omega_n) = \frac{G_d^0}{1 - \frac{t^2}{V} G_0^d \sum_k G_0^c},$$

hence

$$G_d(i\omega_n) = \frac{1}{i\omega_n - \varepsilon_d - \frac{t^2}{V} \sum_k \frac{1}{i\omega_n - \varepsilon_k}}.$$

This expression is similar to the one we obtained previsouly without resorting to a diagrammatic calculation. We can then identify the self-energy by performing the usual analytic continuation $i\omega_n \to \omega + i0^+$.

## 3.8 Electron-phonon interaction

Consider the following Hamiltonian describing the interaction between electrons and phonons

$$\hat{H} = \sum_{k,\sigma} \varepsilon_k \hat{c}^\dagger_{k,\sigma} \hat{c}_{k,\sigma} + \sum_q \omega_q \hat{b}^\dagger_q \hat{b}_q + \sum_q g_q (\hat{b}_{-q} + \hat{b}^\dagger_q) \sum_k \hat{c}^\dagger_k \hat{c}_{k+q}. \tag{3.15}$$

In this Hamiltonian, the first two terms designate the electrons and the phonons respectively, while the $\hat{V}$ interaction is contained in the third term. In the latter, we have on the one hand the Fourier transform of $\hat{\varphi}(x) = \sum_q (\hat{b}_{-q} + \hat{b}^\dagger_q) e^{iqx}$, ans also $\hat{n}_q$ the Fourier transform of the electron density of the system. We will as before write our Hamiltonian in the form of a sum of two terms

$$\hat{H} = \hat{H}_0 + \hat{V},$$

where obviously the bare Hamiltonian is made up of the first two terms of Eq. (3.15).

We will describe this problem in terms of Feynman diagrams. The basic vertex of this problem is depicted in Fig. (3.5.a). However, as we are going to be interested in the electronic Green function, we find that this type of vertex contributes zero when it does appear only once, and only diagrams with an even number of vertex make a non-zero contribution. These vertex are of the form in Fig. (3.5.b).

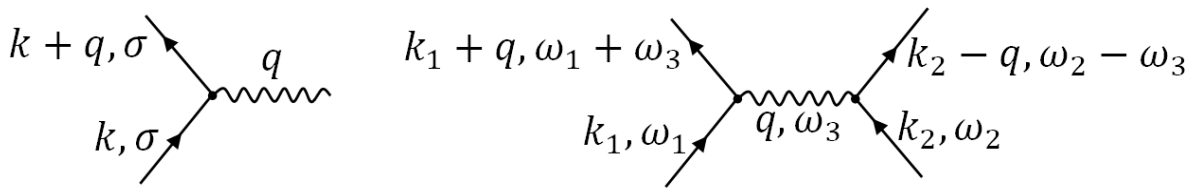


(a) (b)

FIGURE 3.5 – (a) Simple vertex (b) Vertex with a non-zero contribution

The considered interaction is therefore a retarded interaction mediated via a phonon carrying a $q$ wave vector and a frequency $\omega_3$. At each vertex of this type a factor $g_q^2 D_0(q, \omega_3)$ should be associated. The construction rules of the Feynman diagrams are in this case the same as for interacting electrons. In particular the sign of each of the contributions is given by $(-1)^{F+n/2}$ (where $n$ is the number of electron-phonon vertex and $F$ the number of fermionic loops). The bare Green function is given by

$$D_0(q, i\omega_3) = \frac{2\omega_q}{(i\omega_3)^2 - \omega_q^2},$$

while the Green function in the time and position domain is defined by

$$D(x - x', \tau - \tau') = -\left\langle T_\tau \hat{\varphi}(x,\tau) \hat{\varphi}(x',\tau') \right\rangle.$$

### 3.8.1 Electronic self-energy

The lowest order diagrams to be used are of the Fock and Hartree type. The Hartree tree only generates a shift of the chemical potential, and therefore only the Fock term will have a real importance. We will therefore calculate only the contribution of the Fock term to the self energy, that is to say

$$\Sigma_F(k, i\omega_n) = -T \sum_{q, i\nu_n} g_q^2 G_0(k - q, i\omega_n - i\nu_n) D_0(q, i\nu_n), \tag{3.16}$$

that we can write using the explicit form of $G_0$ and $D_0$ as

$$\Sigma_F(k, i\omega_n) = -T \sum_{q, i\nu_n} g_q^2 \frac{1}{i\omega_n - i\nu_n - \varepsilon_{k-q}} \frac{2\omega_q}{(i\nu_n)^2 - \omega_q^2}.$$

The last term corresponding to $D_0$ can be expanded as a sum of simple elements, and we get

$$\Sigma_F(k, i\omega_n) = -T \sum_{q, i\nu_n} g_q^2 \left( \frac{1}{i\omega_n - i\nu_n - \varepsilon_{k-q}} \frac{1}{i\nu_n - \omega_q} - \frac{1}{i\omega_n - i\nu_n - \varepsilon_{k-q}} \frac{1}{i\nu_n + \omega_q} \right). \tag{3.17}$$

On these two terms we observe that we can get one from the other by simply changing $\omega_q$ to $-\omega_q$, and so we can simply focus on the calculation of only one of these terms.

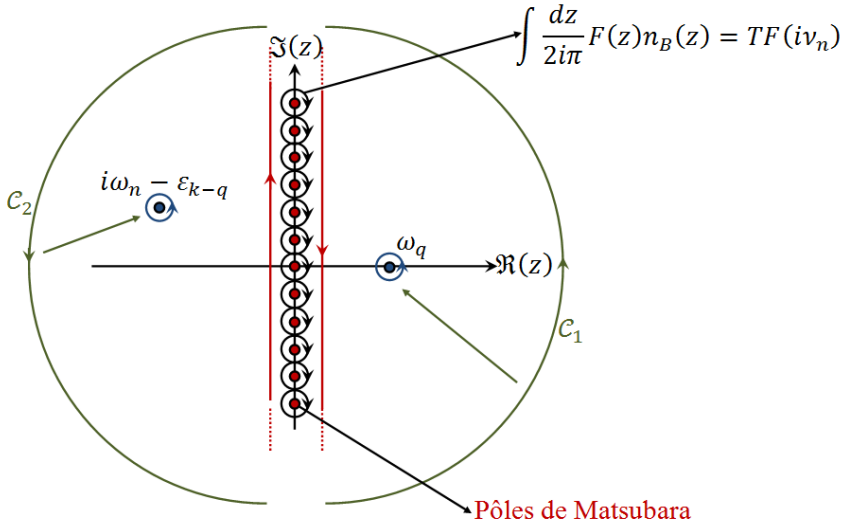


FIGURE 3.6 – Pôles de $F(z)$

We should evaluate a sum like $-T\sum_{i\nu_n} F(i\nu_n)$ corresponding as we have seen previously to a summation on the Matsubara poles of the function $-F(z)n_B(z)$. For bosons, $\text{Res} n_B(z)|_{z=i\nu_n} = T$, whereas for fermions $\text{Res} n_F(z)|_{z=i\omega_n} = -T$. The poles of $F(z)$ are of two types (see Fig. (3.6)). The first ones correspond to the Matsubara frequencies and are purely imaginary. The second ones correspond to the points $i\omega_n - \varepsilon_{k-q}$ and $\omega_q$. The term $TF(i\nu_n)$ corresponds to the integral on a contour represented in black in the figure of the function $F(z)n_B(z)/2i\pi$. By performing a continuous deformation of these contours, we can merge them to obtain a new contour whose shape is represented in red going from $-\infty$ to $+\infty$ on the imaginary axis and remaining close to the origin on the real axis. It is possible to complete this contour with two circular arcs represented here in green. The two contours $\mathcal{C}_1$ and $\mathcal{C}_2$ obtained by joining the red and green contours thus give us contours surrounding the two poles that can be continuously deformed until they form two circles surrounding them (represented in blue). Ultimately, our sum $-T\sum_{\nu_n} F(i\nu_n)$ can be rewritten as

$$\begin{aligned} -T \sum_{\nu_n} F(i\nu_n) &= \int_{\mathcal{C}_1} \frac{dz}{2i\pi} n_B(z) F(z) + \int_{\mathcal{C}_2} \frac{dz}{2i\pi} n_B(z) F(z) \\ &= n_B(\omega_q) \frac{1}{i\omega_n - \omega_q - \varepsilon_{k-q}} - n_B(i\omega_n - \varepsilon_{k-q}) \frac{1}{i\omega_n - \varepsilon_{k-q} - \omega_q} \\ &= \frac{n_B(\omega_q) - n_B(i\omega_n - \varepsilon_{k-q})}{i\omega_n - \varepsilon_{k-q} - \omega_q}. \end{aligned}$$

Note that this result can be obtained directly using the general equation we derived to calculate summation over Matsubara frequencies in Sec. 2.4.3. Using the fact $e^{i\beta\omega_n} = 1$, we can transform the Bose-Einstein distribution into a Fermi-Dirac distribution :

$$n_B(i\omega_n - \varepsilon_{k-q}) = -1 + n_F(\varepsilon_{k-q}).$$

Therefore,

$$-T \sum_{\nu_n} F(i\nu_n) = \frac{n_B(\omega_q) + 1 - n_F(\varepsilon_{k-q})}{i\omega_n - \varepsilon_{k-q} - \omega_q},$$

which provides us finally

$$\Sigma_F(k,i\omega_n) = \sum_q g_q^2 \left[ \frac{n_B(\omega_q) + 1 - n_F(\varepsilon_{k-q})}{i\omega_n - \varepsilon_{k-q} - \omega_q} + \frac{n_B(\omega_q) + n_F(\varepsilon_{k-q})}{i\omega_n - \varepsilon_{k-q} + \omega_q} \right]. \tag{3.18}$$

In this expression, we can identify the first term with an emission phenomenon and the second with an absorption phenomenon.

We will now perform an analytical continuation of our self-energy to obtain $\Sigma_F(k,\omega+i0^+)$, namely we perform the transformation $i\omega_n \to \omega + i0^+$. The imaginary part of $\Sigma_F(k,\omega+i0^+)$ now reads

$$\Im\big[\Sigma_F(k,\omega+i0^+)\big] = -\pi \sum_q g_q^2 \left( [n_B(\omega_q) + 1 - n_F(\varepsilon_{k-q})]\, \delta(\omega - \varepsilon_{k-q} - \omega_q) + [n_B(\omega_q) + n_F(\varepsilon_{k-q})] \delta(\omega - \varepsilon_{k-q} + \omega_q) \right).$$

We will now use the following two identities

$$\begin{aligned} n_B(\omega_q) + 1 - n_F(\varepsilon_{k-q}) &= (1 + e^{-\beta\omega})(1 + n_B(\omega_q))(1 - n_F(\varepsilon_{k-q})) \quad \text{where } \omega = \varepsilon_{k-q} + \omega_q & (3.19) \\ n_B(\omega_q) + n_F(\varepsilon_{k-q}) &= (1 + e^{-\beta\omega}) n_B(\omega_q)[1 - n_F(\varepsilon_{k-q})] \quad \text{where } \omega = \varepsilon_{k-q} - \omega_q. & (3.20) \end{aligned}$$

The imaginary part of the self-energy reads

$$-\Im\big[\Sigma_F(k,\omega+i0^+)\big] = \pi \sum_q g_q^2 (1 + e^{-\beta\omega})(1 - n_F(\varepsilon_{k-q}))\, [(1 + n_B(\omega_q))\delta(\omega - \varepsilon_{k-q} - \omega_q) + n_B(\omega_q)\delta(\omega - \varepsilon_{k-q} + \omega_q)].$$

In the factor $1 + e^{-\beta\omega}$, we have two competing processes, on the one hand the electronic processes and on the other hand the hole processes. Concerning the terms that multiply the Dirac functions, the first is related to an emission process while the second is related to a phonon absorption process. Indeed for the emission $\omega = \varepsilon_{kq} + \omega_q$, an incident electron of energy $\omega$ is diffused and produces an electron of energy $\varepsilon_{kq}$ and a phonon of energy $\omega_q$. On the contrary, in the case of an absorption process $\omega + \omega_q = \varepsilon_{k-q}$, an incident electron of energy $\omega$ and a phonon of energy $\omega_q$ interact to form an electron of energy $\varepsilon_{k-q}$ (here we used the fact that $\omega_q$ is an even function of $q$ due to the Hamiltonian symmetry).

Coming back to our initial self-energy, we have

$$\Sigma_F(k,z) = \sum_q g_q^2 \left[ \frac{1 + n_B(\omega_q) - n_F(\varepsilon_{k-q})}{z - (\varepsilon_{k-q} + \omega_q)} + \frac{n_B(\omega_q) + n_F(\varepsilon_{k-q})}{z - (\varepsilon_{k-q} - \omega_q)} \right].$$

This quantity is in general difficult to evaluate. However we can assume that the $k$ dependence is much weaker than the $\omega$ dependency. Therefore we replace the self-energy by its average over $k$ assuming that the k-dependence is weak or more specifically by its average over energy. We are thus led to define the new quantities $\tilde{\Sigma}_F(z)$ corresponding to the sum over $k$ of $\Sigma_F(k,z)$ :

$$\tilde{\Sigma}_F(z) = \sum_k \Sigma_F(k,z) = \int_{-\infty}^{+\infty} d\varepsilon \rho_0 \int_0^{+\infty} d\nu \alpha^2(\nu) F(\nu) \left[ \frac{1 + n_B(\nu) - n_F(\varepsilon)}{z - (\varepsilon + \nu)} + \frac{n_B(\nu) + n_F(\varepsilon)}{z - (\varepsilon - \nu)} \right], \tag{3.21}$$

where $\rho_0$ is the electronic density of states, $F(\nu)$ is the density of states for the phonons $\sum_q \delta(\nu - \omega_q)$, and $\alpha^2(\nu)$ a function able to keep trace of the $q$ dependency of $g_q^2$.

For the case of phonons $\omega_q = c|q| \geq 0$ which generates the lower bound 0 for the summation over the phonons'energy. At $T = 0$, $n_B(\nu) = 0$ while $n_F(\varepsilon) = \theta(-\varepsilon)$. Our average self-energy then becomes

$$\tilde{\Sigma}_F(z) = \int_0^{+\infty} d\nu \rho_0 \alpha^2(\nu) F(\nu) \ln \left[ \frac{\nu - z}{\nu + z} \right],$$

that we can write as

$$\tilde{\Sigma}_F(\omega) = \tilde{\Sigma}(0) - \lambda\omega, \tag{3.22}$$

where

$$\lambda = -\frac{\partial \Re\tilde{\Sigma}_F}{\partial\omega} = 2\int_0^{+\infty} d\nu \rho_0 \frac{\alpha^2(\nu) F(\nu)}{\nu},$$

whose value is of order 0.1 or 0.2 for metals.

### 3.8.2 Electronic Green functions

We can then write our Green function for electrons

$$G(k,\omega+i0^+) = G^R(k,\omega) = \frac{1}{\omega-\varepsilon_k-\tilde{\Sigma}_F(\omega)} = \frac{1}{\omega-\varepsilon_k^*-\lambda(\omega-\varepsilon_k^*)+i\Gamma}, \tag{3.23}$$

where we defined

$$\begin{aligned} \varepsilon_k^* &= \varepsilon_k + \Re\tilde{\Sigma}_F(\varepsilon_k^*) \\ \Gamma &= -\Im\tilde{\Sigma}_F. \end{aligned}$$

We can finally put our Green function in the form

$$G^R(k,\omega) = \frac{Z}{\omega-\varepsilon_k^*+i\Gamma^*}, \tag{3.24}$$

where $Z = \frac{1}{1+\lambda} < 1$ et $\Gamma^* = \Gamma Z$.

We can infer from this expression the effective mass $\frac{d\varepsilon_k}{d\varepsilon_k^*} = \frac{m^*}{m} = 1+\lambda > 1$. The quantity $Z$ corresponds (at $T=0$) to a jump in the density of states $n_k$ at the Fermi wave vector $k_F$ generated by the electron-phonon coupling (see Fig. 3.7).

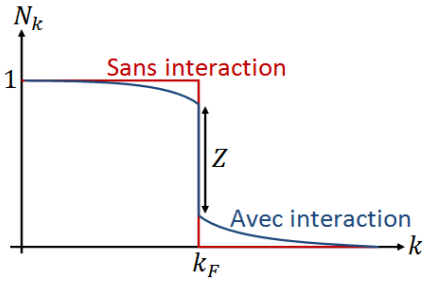


FIGURE 3.7 – Electronic density at $T=0$ with an electron-phonon coupling.

This is then possible to determine the heat capacity $C = \gamma^* T$ where $\gamma^* = \frac{\pi^2}{3}k_B^2 N^*(0)$ with $N^*(0) = N(0)(1+\lambda)$. The density of state is therefore proportional to the mass.

### 3.8.3 Phononic Green functions

We just see in the previous section how the single particle Green function is dressed by phonons. We can obviously wonder how the single phonon propagator is dressed by the electrons.

The lowest non-zero diagram for the phonon propagator is sketched in Fig. 3.8.

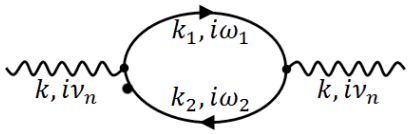


FIGURE 3.8 – Second order diagram of the phonon propagator renormalized by the electrons

Energy and momentum conservation imply $i\nu_n = i\omega_1 - i\omega_2$ and $\mathbf{k} = \mathbf{k}_1 - \mathbf{k}_2$.

If we call $D(\mathbf{k}, i\nu_n)$ the renormalized phonon propagator and $D_0(\mathbf{k}, i\nu_n)$ the bare one, we have

$$D(\mathbf{k},i\nu_n) = D_0(\mathbf{k},i\nu_n) + D_0(\mathbf{k},i\nu_n)\Pi(\mathbf{k},i\nu_n)D_0(\mathbf{k},i\nu_n) + D_0(\mathbf{k},i\nu_n)\Pi(\mathbf{k},i\nu_n)D_0(\mathbf{k},i\nu_n)\Pi(\mathbf{k},i\nu_n)D_0(\mathbf{k},i\nu_n) + \cdots$$

We can resum the series to write

$$D(\mathbf{k}, i\nu_n) = \frac{D_0(\mathbf{k}, i\nu_n)}{1 - \Pi(\mathbf{k}, i\nu_n) D_0(\mathbf{k}, i\nu_n)},$$

where $\Pi(\mathbf{k}, \nu_n)$ corresponds to a fermionic contribution to the phonon self-energy. We already met $\Pi$ before because $\Pi$ corresponds to a four-point fermionic correlation function and more precisely to a density-density correlator.

Using the notation of Fig. 3.8,

$$\Pi(\mathbf{k}, \nu_n) = \frac{1}{\mathcal{V}\beta} \sum_{\mathbf{k}_1, i\omega_{1,n}} |g_q|^2 G_0(\mathbf{k}_1, i\omega_{1,n}) G_0(\mathbf{k}_1 - \mathbf{k}, i\omega_{1,n} - i\nu_n).$$

The calculation of $\Pi(\mathbf{k}, \nu_n)$, the so-called fermionic bubble will be done in the exercice part.

# Chapitre 4

# Introduction to quantum impurity models

## 4.1 Anderson and Kondo models

Quantum impurities take place when a finite size quantum system couples to a free electron bath. Historically, this applies to atomic impurities in metals. However, the above definition is quite general and encapsulates all sorts of defects in a bath. Therefore the number of models which could describe such system is quite large. However, as usual we rely on a few paragdigmatic models which are to play a key pivotal role in our understanding of this physics. The first of these models is the **Anderson model** whose Hamiltonian is written

$$\hat{H} = \sum_{k,\sigma} \varepsilon_k \hat{c}^\dagger_{k,\sigma} \hat{c}_{k,\sigma} + \sum_\sigma \varepsilon_d \hat{d}^\dagger_\sigma \hat{d}_\sigma + U \hat{n}_{d\uparrow} n_{d\downarrow} + \sum_{k\sigma} \Big( V_k \hat{c}^\dagger_{k,\sigma} \hat{d}_\sigma + \text{h.c.} \Big). \tag{4.1}$$

This Hamiltonian describes the interaction between an electronic bath represented by the creation operators $\hat{c}$ and a discrete level represented by the creation operators $\hat{d}$. These two states interact via a term $V_k$ which couplies states $|c, k\sigma\rangle$ and $|d, \sigma\rangle$. The interaction within each of these states is contained for the bath by the kinetic energy $\varepsilon_k$ and for the discrete state by the kinetic energy $\varepsilon_d$ to which we add a Coulomb-like interaction between the electrons of different spins via the energy $U$. Notice that we already met the Anderson model but at $U = 0$.

The second model we will encounter is the Kondo model which describes a magnetic impurity. The Hamiltonian reads :

$$\hat{H} = \sum_{k,\sigma} \varepsilon_k \hat{c}^\dagger_{k,\sigma} \hat{c}_{k,\sigma} + J_K \sum_{k,k'} \hat{\vec{S}} \hat{c}^\dagger_k \vec{\sigma} \hat{c}_{k'} + h \hat{S}^z + h \sum_k \hat{c}^\dagger_k \sigma^z \hat{c}_k. \tag{4.2}$$

Here, the bath is coupled to a spin $\hat{\vec{S}}$ with the Kondo coupling energy $J_K$. This is a local magnetic exchange interaction between the bath and a magnetic impurity localized say in $\vec{r} = 0$. This Hamiltonian also includes the interaction with a magnetic field $h$. The impurity is assumed to be at rest, therefore its kinetic energy is not taken into account.

There are many other variants and extension of this model. In particular, we can consider large spin $S > 1/2$, by increasing the number of orbitales $|d\rangle$ (in the Anderson model) or by increasing the number of impurities (in the Kondo model). One can also take into account, some internal degrees of freedom in the bath which increases the numbe rof independent channels that couples to the impurity. As we will see, this leads to highly non-trivial physics which will push us away from the Fermi-liquid paradigm.

These systems are correlated systems contrasting with the case of the one-body problem where the Hamiltonian reads

$$\hat{H} = \sum_{k,\sigma} \varepsilon_k \hat{c}^\dagger_{k,\sigma} \hat{c}_{k,\sigma} + \sum_{kk'} V_{kk'} \hat{c}^\dagger_k \hat{c}_{k'}$$

The single-particle problem is trivially solved by exact diagonalization. However, the Anderson and Kondo problem belong to many-bodu problems. Let us consider the case of the Kondo model with the isolated spin in a $\sigma$ orientation coupled to the bath. If an electron interacts with this spin, this spin can, because of the term $J_k \hat{c}^\dagger \hat{\vec{S}} \cdot \vec{\sigma} \hat{c}$, modify its orientation. If a second electron interacts later with this spin, its orientation having been modified, this will

further induce correlations between the two electrons in an indirect way. The spin-flip induces correlations between electrons all together.

## 4.2 Physical Motivation

### 4.2.1 Magnetic impurities in a metal

The presence of magnetic impurities in a metal can have physical consequences. Indeed, it has been measured in experiments as early as the 1930s that the low temperature resistivity of certain metals, instead of uniformly tending toward a minimum value $\rho_0$ at zero temperature, showed a rise in resistivity. Indeed, in the case of Fermi liquids where the interactions are between electrons, the behavior of the resistivity is in $T^2$, whereas for the case of interaction via phonons, the evolution is done in $T^3$. The relative difference measured between $\rho_0$ and this new resistivity is of the order of 1 to 4%. This is thus a small and extremely reproducible shift. This behavior can in particular be observed in the case where a metal like $Cu$ has $Mg$ magnetic impurities.

This behavior was explained by Kondo in 1964 [4]. It thus determines the temperature scale $T_K$ from which the resistivity starts to leave the behavior in $T^n$ as a function of the interaction parameters of the Hamiltonian in (4.2).

### 4.2.2 Quantum dots

The theory of transport in quantum dots dates back to 1988 . The experimental realization of the Kondo effect in quantum dots dates follows ten years later in 1998. A simple Hamiltonian able to describe such system can be written as

$$\hat{H} = \sum_{\sigma,\alpha} \varepsilon_k \hat{c}_{k,\alpha,\sigma} \hat{c}_{k,\alpha,\sigma} + \varepsilon_d \hat{d}^\dagger \hat{d} + \sum_{k,\sigma,\alpha} (V_k \hat{c}^\dagger_{k\alpha\sigma} \hat{d}_\sigma + \text{h.c.}),$$

where $\alpha$ denotes the left or right electrode and $\hat{d}^\dagger$ is the creation operator of an electron in the quantum dot (see FIGURE (4.1)). This system is thus described by a Hamiltonian close to Anderson's Hamiltonian. The theoretical problem in these systems will be to determine the current $I$ in response to a voltage $V$ as well as the correlations $\langle II \rangle$. One can observe similar transport observables when a molecule is inserted between two electrodes.

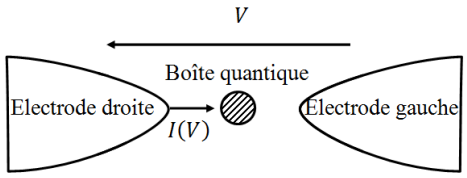


FIGURE 4.1 – Scheme of a quantum dot

These days, some highly asymmmetric mixture of cold atoms may also offer a description of such system.

### 4.2.3 Theoretical motivation : Dynamical mean field theory

The Ising model is well known in statistical physics. The Ising Hamiltonian

$$H = -J \sum_{ij} S_i S_j.$$

can be solved approximately using a mean field theory approach which was first introduced by [5]. In the mean field approximation, the effective Hamiltonian reads

$$H_{eff} = -h_{eff} S,$$

where $h_{eff}$ denotes the effective magnetic field created by the neighbours of $S$. To this Hamiltonian, it is necessary to add a condition of self-consistency by writing the effective field as a function of the mean spin

$$h_{eff} = f(\langle S \rangle).$$

Let us assume we want to follow the same strategy to solve the Hubbard model. The quantum analogue of the Hubbard model in the dynamic mean field approach becomes an Anderson impurity model with self-consistency conditions via effective energies $V^{eff}$ and $\varepsilon_d^{eff}$. We then find ourselves in the presence of an effective electron bath. Therefore, within this approximation, the Anderson model becomes the central ingredient. Therefore, it is crucial to develop some effcient numerical solution of the Anderson model (called an impurity solver) in order to use it as the core in a DMFT approach.

## 4.3 Anderson model

### 4.3.1 Atomic limit

The atomic limit corresponds to $V_k = 0$. In this limit, the Anderson Hamiltonian reads

$$\hat{H} = \sum_\sigma \varepsilon_d \hat{d}^\dagger_\sigma \hat{d}_\sigma + U \hat{n}_{d\uparrow} \hat{n}_{d\downarrow}.$$

We then have four eigenstates that are formed from the different spin states allowed by Pauli's principle,

$$|0\rangle, |\uparrow\rangle, |\downarrow\rangle, |\uparrow\downarrow\rangle.$$

The first of these states has zero energy, the second one (degenerate with the third) has a $\varepsilon_d$ energy and the last one has an energy $2\varepsilon_d + U$ energy. The density of states of such a system consists of a set of peaks located at energies corresponding to the energy difference between two states whose number of particles differs from 1. In this case, we would have two peaks (of modulated amplitude) located at the energy $\varepsilon_d$ and $\varepsilon_d + U$.

The number of particules in a given spin state is given by

$$n_\sigma = \frac{n_d}{2} = \frac{n_{d\uparrow} + n_{d_\downarrow}}{2} = \frac{e^{-\beta\varepsilon_d} + e^{-\beta(2\varepsilon_d+U)}}{1 + 2e^{-\beta\varepsilon_d} + e^{-\beta(2\varepsilon_d+U)}}.$$

The energy dependence of this distribution is represented on the FIGURE (4.2)

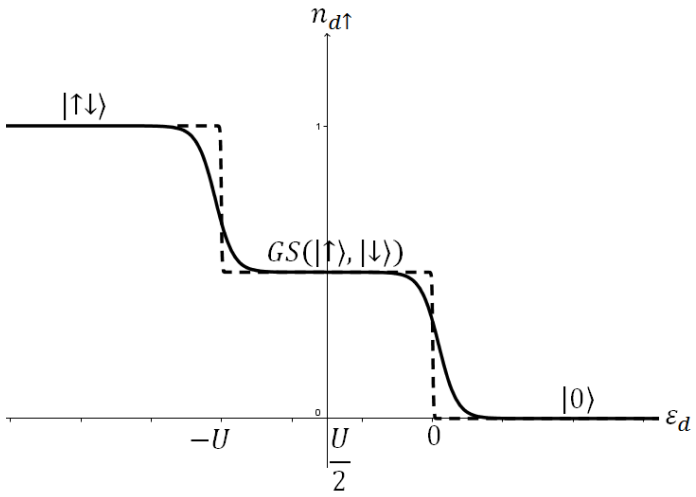


FIGURE 4.2 – Number of particles with spin $\uparrow$ as a function of $\varepsilon_d$ in the atomic limit of the Anderson model. The dashed line is the limit $T \to 0$.

Between $\varepsilon_d = -U$ and $\varepsilon_d = 0$, the system is in the local moment regime where the ground state contains one electron. For $S = 1/2$ we can then ask ourselves what is the Hamiltonian that will be obtained in the limit $U \to \infty$ and $\varepsilon_d \to -\infty$ when the coupling to the bath $V$ is switched on. One can therefore treat this coupling in perturbation theory and projects the obtained Hamiltonian in the $n_d = 1$ state. One obtains an effective Hamiltonian which reads

$$\hat{H}_{eff} = \sum \varepsilon_k \hat{c}^\dagger_{k\sigma} \hat{c}_{k\sigma} + \sum_k J_{kk'} \hat{c}^\dagger_{ks} \hat{\vec{S}} \cdot \frac{\vec{\sigma}_{ss'}}{2} \hat{c}_{k's'} + \sum_{k,k',s} \bar{V}_{kk'} \hat{c}^\dagger_{k,s} \hat{c}_{k's}. \tag{4.3}$$

Notice that the term containing the spin $\vec{S}$ is the only one allowed by the SU(2) symmetry. As for the term $\bar{V}$, this is a scalar term that will be neglected because it does not bring further correlations.

In order to relate the coupling $J_{kk'}$ of the Kondo Hamiltonian to the parameters of the Anderson Hamiltonian, we can perform a second order perturbative calculation in $V$. We therefore have to calculate the effect of the process depicted in Fig. 4.3. The difference in energy between the ground state and the excited states $|0\rangle$ and $|\uparrow\downarrow\rangle$ are $(E_0 - E_1) \approx \varepsilon_F - \varepsilon_d$ and $(E_2 - E_1) \approx \varepsilon_d + U - \varepsilon_F$ respectively. We therefore obtain at second order

$$J_K \equiv J_{kk'} \approx V^2 \left( \frac{1}{\varepsilon_d + U - \varepsilon_F} + \frac{1}{\varepsilon_F - \varepsilon_d} \right) \tag{4.4}$$

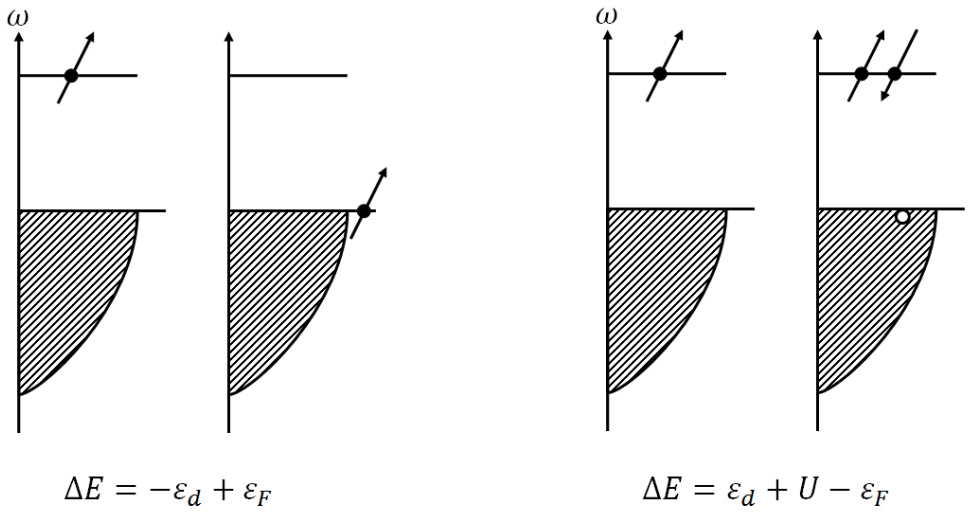


FIGURE 4.3 – In order to determine the expression of $J_K$ at second order in perturbation theory, we shall find the energy difference between the ground states $|\uparrow\rangle, |\downarrow\rangle$ and the excited states $|\uparrow\downarrow\rangle$ et $|0\rangle$.

## 4.4 Summary of the main results related to the Kondo model

### 4.4.1 Perturbative approach

The resolution of the Kondo model goes through a perturbative analysis in $J_k$. From these calculations, we can determine the susceptibility, the heat capacity and the resistivity as

$$\chi_{imp} = (g\mu_B)^2 \frac{S(S+1)}{3T}\left(1 - 2J_K\rho_0 - (2J_K\rho_0)^2 \ln\frac{D}{T}\right) \tag{4.5}$$

$$C_{imp} = \pi^2 S(S+1)(2J\rho_0)^4\left(1 + 8J\rho_0 \ln\frac{D}{T}\right) \tag{4.6}$$

$$R_{imp} = \frac{3\pi mS}{2e^2\hbar\varepsilon_F}\left(J^2 + 4J^3\rho_0 \ln\frac{D}{T} + \cdots\right), \tag{4.7}$$

where $D$ is the band width and $\rho_0$ the density of states at the Fermi level. We find in each of these terms a logarithmic dependence diverging at zero temperature and when sending $D \to \infty$. This divergence is an artefact of the perturbative expansion and is cured by the terms of higher order. However, this calculation first performed by Kondo pridcts correctly a rise of the resistivity as observed experimentally.

Excercice : Can you recover the first two terms in the expansion of $\chi_{imp}$ in Eq. (4.5) ?

Notice that all the above expressions can be rewritten in terms of some effective coupling

$$J_{eff}(D) = J\rho_0\left(1 + 2J\rho_0 \ln\frac{D}{T}\right).$$

If we make this substitution, the thermodynamic quantities depend only on $J_{eff}(D)$ and the divergences disappear : they are absorbed by the redefinition of the Kondo coupling which now beomes scale-dependent. The divergence results from an inconsistency of the perturbative expansion in which the term of first order becomes larger than the term of order 0. This will clearly be the case if the temperature is very small. However this is not the case if the temperature is extremely large $k_BT \lesssim D$ in which case the pertubative expansion makes sense and is controlled. One can thus determine a limiting temperature, called **Kondo temperature** below which these expressions are not valid any more. The Kondo temperature is defined as

$$2J\rho_0 \ln\frac{D}{T_K} = 1,$$

which provides

$$T_K = De^{-\frac{1}{2J\rho_0}}. \tag{4.8}$$

We therefore have two different temperature regimes $T \ll T_K$ and $T \gg T_K$. These regimes are not separated by a phase transition. $T_K$ corresponds to a crossover scale separating these two regimes. At large $T \gg T_K$, we have essentially a free spin and therefore a Curie law. Eventually, we can resum the perturbative series of the logarithmic divergence (see Fig. 4.4). However, the perturbative calculation of Kondo does not explain the behaviour at low temperature. This corresponds to the strong coupling regime in which we have the impression that the effective Kondo coupling grows infinitely. However, this cannot be the case. Actually, if we set $J_K \to \infty$ in the original Kondo model, the physics is quite clear. The ground state is obtained when one electron forms a singlet with the spin of the impurity and therefore screens it. Once screened, we expect to recover a Fermi liquid behavior. This is actually what is found. Therefore, at low T, we expect to recover a Pauli susceptibility because the impurity has been screened. The expected qualitative behavior is this sketched in Fig. 4.4.

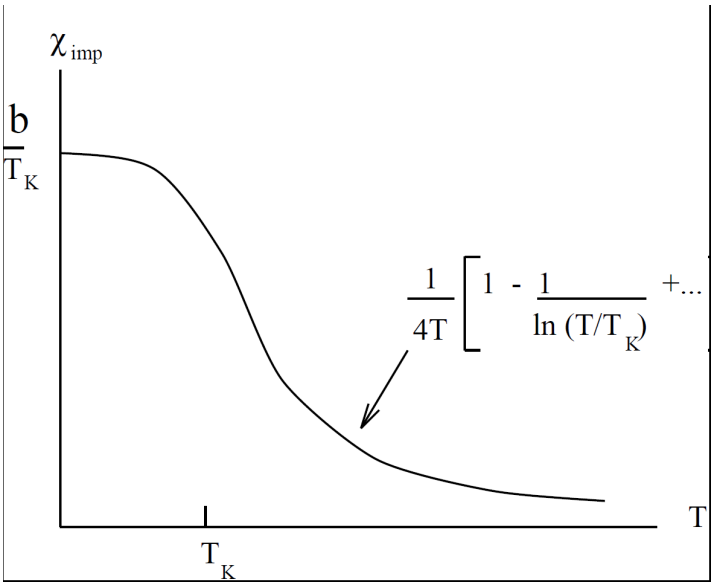


FIGURE 4.4 – Qualitative behaviour of the impurity susceptibility $\chi_{imp} = \chi_{tot} - \chi_{Pauli}$ with temperature.

One can perform the same analysis for the other quantities such as the resistivity or the specific heat. The Fermi-liquid approach to the strong coupling fixed point of the Kondo problem was developed by Nozieres in 1974 [6] in a very elegant and thoughful paper. We won't develop it here though we have all tools to do it.

### 4.4.2 Renomalization group and universality

The above perturbative suggests to absorb the logarithmic divergences with a redefinition of the Kondo coupling :

$$J_{eff}(D) = J\rho_0 \left(1 + 2J\rho_0 \ln \frac{D}{T}\right).$$

The Kondo coupling becomes scale-dependent. This suggests to use the renormalization group (RG) to the Kondo problem. The idea of the RG is integrate out the conduction electron $c_k$ for $k$ far from $k_F$, the Fermi wave-vector, and successively reduce the band-width $D$ to obtain a new effective interaction. [See Figure (4.5).] This is hard to do exactly. At weak coupling one can do it perturbatively in the dimensionless coupling $\lambda = 2J\rho$.

This is equivalent to renormalize the Kondo interaction. This calculation will be done as an exercice at the end of this chapter. We find

$$\lambda(D') = \lambda(D)\lambda^2 \ln(\frac{D}{D'}).$$

Writing $D = D' + \delta D$ with $\delta D \ll D$, we obtain a differential equation for $\lambda$

$$\frac{d\lambda}{d\ln D} = -\lambda^2. \tag{4.9}$$

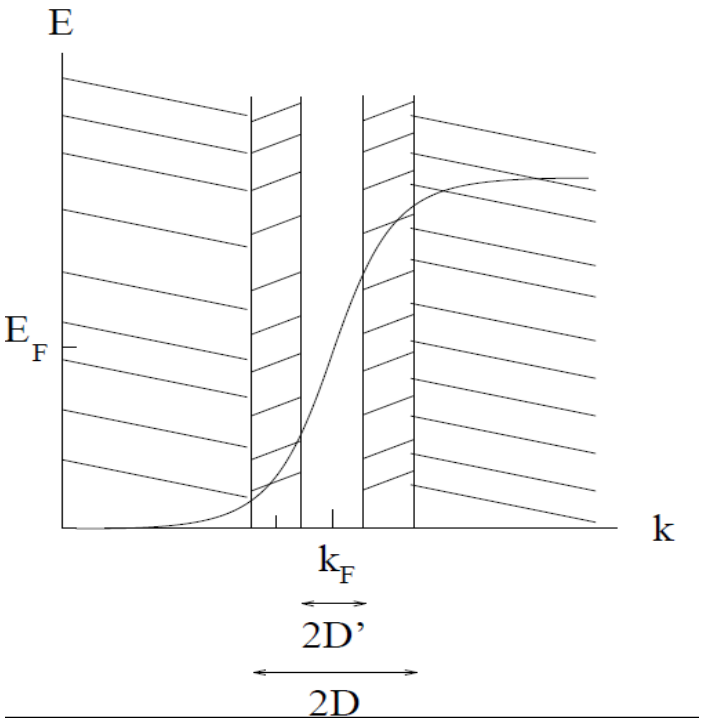


FIGURE 4.5 – Reduction of the cut-off from $D$ to $D'$.

We see that lowering the band cut-off increases $\lambda$ or, defining a length-dependent cut-off, $l \sim v_F/D$, the equation becomes

$$\frac{d\lambda}{d\ln l} = \lambda^2. \tag{4.10}$$

Integrating the equation (this is equivalent to performing an infinite sum of diagrams), gives :

$$\lambda_{\text{eff}}(D) = \frac{\lambda_0}{1 - \lambda_0 \ln \frac{D_0}{D}}. \tag{4.11}$$

If $\lambda_0 > 0$ (antiferromagnetic interaction), then $\lambda_{\text{eff}}(D)$ diverges (typically becomes of order $O(1)$ and thus uncontrolled) at the scale $D \sim T_k \sim D_0 e^{-\frac{1}{\lambda_0}} = D_0 e^{-\frac{1}{2J\rho_0}}$. If $\lambda_0 < 0$ (ferromagnetic interaction), $\lambda_{\text{eff}}(D) \to 0$. We can represent this behavior as a 1D flow of renormalization as sketched in Figure (4.6).

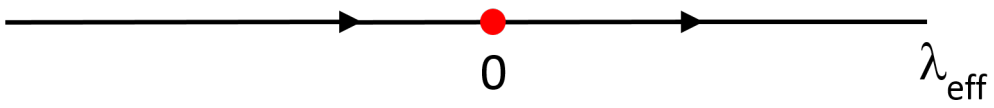


FIGURE 4.6 – RG flow of the Kondo coupling.

From the flow depicted in Fig. 4.6 the Kondo coupling grows when the scale $D$ decreases (i.e. in the infrareed limit). Conversely, at high energy the Kondo coupling goes to zero. Therefore, in the high energy limit, the system becomes asymptotically free. This concept is called asymptotic freedom. This is a property of some gauge theories that causes interactions between particles to become asymptotically weaker as the energy scale increases and the corresponding length scale decreases. Asymptotic freedom is a feature of quantum chromodynamics (QCD), the quantum field theory of the strong interaction between quarks and gluons, the fundamental constituents of nuclear matter. Quarks interact weakly at high energies, allowing perturbative calculations.

Another remarkable consequence of the RG flow is that all thermodynamical observable depends on a single variable $\mathcal{O}(T) = f(T/T_K)$ where $f$ is a universal scaling function. Therefore, if we measure the susceptibilities for

different samples with different impurities, on the measurements should rescale on a single universal curve provided we plot them as a function of $T/T_K$. If a magnetic field is added to the system, then the observable becomes a 2-parameter scaling function $\mathcal{O}(T) = g(T/T_K, H/T_K)$.

For impurities in metals, the Kondo temperature depends on the type of impurities and of the density of states. It can be a few Kelvins or tens of Kelvin in metals. In quantum dots, the Kondo temperature if of order of the Kelvin.

We start from a isotropic Kondo interaction to derive these results. One may wonder if these results survive if we break the spin $SU(2)$ rotation symmetry. A general anisotropic Kondo interaction can be written as

$$H_K^{ani} = J_z \hat{S}^z \hat{c}^\dagger(0)\sigma^z \hat{c}(0) + J_\perp(\hat{S}^+ \hat{c}_\downarrow^\dagger(0)\hat{c}_\uparrow(0) + \hat{S}^- \hat{c}_\uparrow^\dagger(0)\hat{c}_\downarrow(0)).$$

Exercice Show that for $J_\perp = J_z$, you recover the isotropic Kondo Hamuiltonian

Introducing the dimensionless Kondo coupling $\lambda_{z/\perp} = 2\rho_0 J_{z/\perp}$, one can derive the following RG equations :

$$\frac{d\lambda_z}{d\ln l} = \lambda_\perp^2, \tag{4.12}$$

$$\frac{d\lambda_\perp}{d\ln l} = \lambda_\perp \lambda_z. \tag{4.13}$$

One can notice that if $J_\perp = 0$, the system does not flow. There is no divergence. Indeed, this corresponds to an Ising like interaction. This shows that this is really the spin-flip term that drives the system to the strong coupling.

Exercice Integrate the above system of differential equations and plot the 2D flow of renormalization. Hint : It is like a Kosterlitz-thouless flow. What happens if we start with different initial coupling $J_z \neq J_Perp$ in the infrared limit ?

### 4.4.3 Multi-channel Kondo model

I will follow here the review of Affleck [7]. Normally there are several “channels" of electrons e.g. different d-shell orbitals. A very simple and symmetric model is :

$$H = \sum_{\vec{k},\alpha,i=1,2,\ldots k} \epsilon_{\vec{k}} \psi_{\vec{k}}^{\dagger\alpha i} \psi_{\vec{k}\alpha i} + \lambda \vec{S} \cdot \sum_{\vec{k},\vec{k}'\alpha,\beta i} \psi_{\vec{k}}^{\dagger\alpha i} \vec{\sigma}_\alpha^\beta \psi_{\vec{k}'\beta i}, \tag{4.14}$$

where $k$ denotes an extra “channel” quantum number. This model has $SU(2) \times SU(k) \times U(1)$ symmetry. Realistic systems do not have in general this full symmetry. However, this model turn out to be very useful to classify the different possible behavior that can occur when a impurity of spin $S$ coupled to k-channels of electron.

Perturbation theory in $\lambda = 2\rho_0 J$ is similar to the result mentioned before. The RG equation reads

$$\frac{d\lambda}{d\ lnD} = -\lambda^2 + \frac{k}{2}\lambda^3 + O[ks(s+1)\lambda^4] \tag{4.15}$$

There are many things we can extract from the flow equation particularly in the large $k$ limit. Indeed, the above differential equations predict a fixed point in $\lambda = 0$, $\lambda \to +\infty$ but also some intermediate fixed point at $\lambda_c = 2/k$. The point is that in the large $k$ limit, such fixed point is still within reach of perturbation theory. We can analyze its stability. The $\beta$-function is $\beta = \lambda^2 - \frac{k}{2}\lambda^3 + O(\lambda^4)$. The slope of the $\beta$-function at the critical point is given by :

$$\left.\frac{d\beta}{dk}\right|_{\lambda_c} = 2\lambda_c - \frac{3}{2}\lambda_c^2 = -\frac{2}{k} < 0. \tag{4.16}$$

This implies that the fixed point is stable in this large $k$ limit. The RG flow is depicted in Fig. 4.7.

Furthermore, the way the flow approaches this fixed point is non-standard. The leading irrelevant coupling constant at the non-trivial (infrared) fixed point has dimension 2/k at large k, so that $(\lambda - \lambda_c)$ scales as $\Lambda^{2/k}$. This is not an integer. This implies that this critical point is not a Fermi liquid !

This approach is only valid in the large k limit. One may also learn of what is going on by taking the limit $\lambda \to \infty$ as $T \to 0$ and check the consistency. What is the groundstate for the lattice model generalized to arbitrary $k$ and $s$, at $\lambda/t \to \infty$ ? In the limit we just consider the single-site model

$$H = J\vec{S} \cdot \psi_0^\dagger \frac{\vec{\sigma}}{2} \psi_0, \tag{4.17}$$

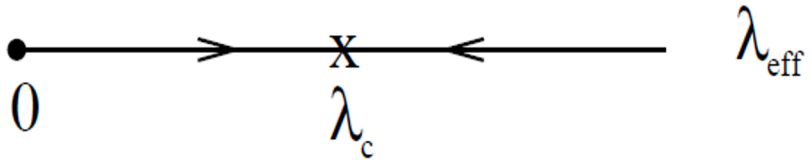


FIGURE 4.7 – RG flow of the Kondo coupling in the overscreened case.

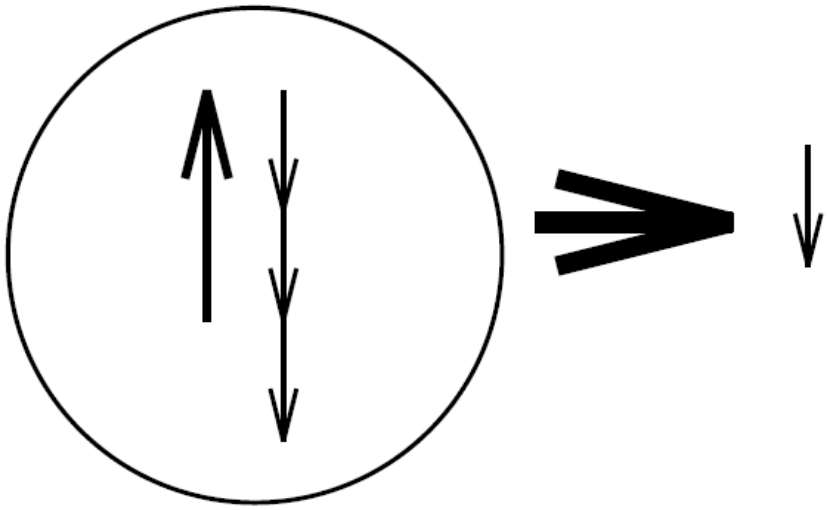

FIGURE 4.8 – Formation of an effective spin at strong Kondo coupling. $k = 3$, $s = 1$ and $s_{\text{eff}} = 1/2$.

For $J > 0$ (antiferromagnetic case) the minimum energy state has maximum spin for electrons at $\vec{0}$ i.e. spin $= k/2$. Coupling this spin-k/2 to a spin-s, we don't get a singlet if $s \neq k/2$, but rather an effective spin of size $|s - k/2|$ [See Figure (4.8)]. The impurity is thus underscreened if $(k/2 < s)$ or overscreened if $(k/2 > s)$.

This leads to two completly different type of physics. In the first (underscreened) case, by performing a strong coupling analysis (perturbation theory in $t/J$ assuming $J \gg t$, one can convince oneself that the hypothesis $J \to \infty$ is stable (more specically, one can show that the residual exchange interaction in $t^2/J$ is ferromagnetic). Therefore the strong coupling fixed point is stable. In this case we expect the infrared fixed point to correspond to a decoupled spin of size $s_{\text{eff}} = s - k/2$ and free electrons (actually with a $\pi/2$ phase shift).

The situation is drastically for the overscreened case. Take for example $k = 2$ and $S = 1/2$. There are two electrons whcih want to form a singlet with the impurity spin. The problem is somehow frustrated. Indeed, the residual exchange interaction in $t^2/J$is antiferromagnetic and therefore wants also to flow to strong coupling. So the hypothesis $J \to +\infty$ is unstable in that case. Therefore they must be some intermediate fixed point which is the one capured in the RG equation in the large k-limit.

Many approaches were used to develop to solve that problem. The k-channel Kondo effect is in fact integrable using the Bethe-Anzatz. However, from this approach this is not so easy to compute some correlation functions. A elegant approach was developed by Affleck and Ludwig in the 90s using boundary comformal field theory (see [7]) which allows to determine analytically the spectrum, the thermodynamical and transport obervables, etc. For example the impurity susceptibility scales as

$$\chi_{\text{imp}} = \left(\frac{1}{T}\right)^{\frac{k-2}{k+2}},$$

which confirms the non-Fermi liquid behavior. An interesting quantity is the impurity entropy

$$S_{\rm imp} = \ln\left(\frac{\sin[\frac{\pi(2S+1)}{k+2}]}{\sin[\frac{\pi}{k+2}]}\right).$$

For example, if we choose $S = 1/2$ and $k = 1$, we find that $S_{\rm imp} = 0$ which means that the spin impurity is completely screened. Instead for $S = 1/2$ and $k = 2$, we find $S_{\rm imp} = \ln 2/2$, i.e. one half of the impurity entropy of spin 1/2. Actually, .this corresponds to the impurity entropy of a free Majorana fermion ! This is not by chance. The 2-channel Kondo fixed point offers a description in terms of a free Majorana fermion (half a fermion).

A complementary approach uses the numerical renormalization group but is limited ot three maybe channels these days. Some very recent experiments with quantum dots have recently confirmed the behavior for the 2-channel Kondo effect and also the 3-channel Konfo fixed point.

## 4.5 Back to the Anderson model

### 4.5.1 $U = 0$

Let us go back to the Anderson model described by the Hamiltonian

$$\hat{H} = \sum_k \varepsilon_k \hat{c}^\dagger_{k,\sigma}\hat{c}_{k,\sigma} + \varepsilon_d \hat{d}^\dagger_\sigma \hat{d}_\sigma + U\hat{n}_{d\downarrow}\hat{n}_{d\uparrow} + \sum_k (V_k \hat{c}^\dagger_{k,\sigma}\hat{d}_\sigma + \text{h.c.}),$$

We are interested in this section to the density of states or spectral function $\rho_d = \langle \hat{d}\hat{d}^\dagger\rangle$.

Let us remind what we found for $U = 0$ and $V \neq 0$. The Matsubara Green function $G_d(i\omega_n)$ reads

$$G_d^{-1}(i\omega_n) = i\omega_n - \varepsilon_d - \Sigma_d(i\omega_n),$$

where

$$\Sigma_d(i\omega_n) = \sum_k |V_k|^2 \frac{1}{i\omega_n + \mu - \varepsilon_k}$$

denotes the self-energy. Therefore, in the $U \to 0$ limit, we expect the dot density of states (DOS) to be peaked at $\omega = \varepsilon_d - \Sigma'(0)$ with a Lorentzian shape of width $\Gamma = \pi V^2 \rho_0$.

### 4.5.2 $U \neq 0$, $V = 0$

We also already discussed the case $U \neq 0$ and $V_k = 0$. At the particle-hole symmetry point, $\varepsilon_d = -U/2$, the Hamiltonien reads

$$\hat{H} = \left(\hat{n}_\uparrow - \frac{1}{2}\right)\left(\hat{n}_\downarrow - \frac{1}{2}\right)U.$$

Our spectral function is then composed of two peaks centered around the energy differences between the different spin states (triplets and singlet) of the system, therefore at $\pm U/2$. When particle/hole symmetry is broken, we expect two peaks located at $\omega = \varepsilon_d$ and $\omega = \varepsilon_d + U$. When $\Gamma$ is very small, we expect these peaks to broaden.

### 4.5.3 General case

The previous limiting case ignore the physics of the Kondo effect. Nevertheless, we know that $\int \rho_d(\omega)d\omega = 1$. Therefore, if something changes in the local DOS, this must be accompagnied with some transfer of spectral weight.

Let us focus on the p/h symmetric case. We know that at $T \ll T_K$, the impurity is screened by the conduction electrons at the Fermi level forming a singlet state. The Fermi liquid is recovered. Therefore such screening process implies it takes many states at the Fermi level to screen the impurity (remmeber this is a many-body screening here). We thus expect a resoannce to occur at teh Fermi level. What could be the width of this Fermi level. The only scale available is $T_K \lesssim \Gamma$. Therefore, we expect that at $T \leq T_K$, or spectral function to be composed of two Hubbard bands located in $\pm U/2$ and a Kondo peak at $\omega = 0$. This quasi-particle resonance is called the Abrikosov-Suhl resonance or Kondo resoannce in the literature. The width of the resonance is given by $\simeq T_K$ while its height is independent of $U$. We have ploted what the local DOS should look like in Fig. 4.9.

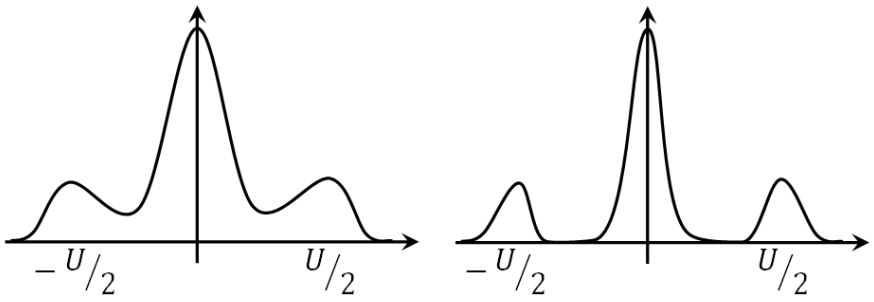


FIGURE 4.9 – Evolution of the de nsity of states with $U$.

## 4.6 Kondo effect in quantum dots

### 4.6.1 Current through a quantum dot

Let us now consider the case of a quantum dot, a system consisting of two electrodes L and R coupled to a dot (denoted by d). The Hamiltonian of this system is

$$\hat{H} = \sum_{k,a} \varepsilon_{k\alpha} \hat{c}^\dagger_{ka} \hat{c}_{ka} + \sum_k \Big( V_{ka,n} \hat{c}^\dagger_{ka} \hat{d}_n + \text{h.c.} \Big) + \hat{H}_{dot}(\hat{d}^\dagger_n, \hat{d}_n), \tag{4.18}$$

The Hamiltonian of the dot, $\hat{H}_{dot}$, can be quite general at this stage. We are interested in the current $\langle I \rangle$ as a function of the chemical potential difference $\mu_L - \mu_R$. The current in the $a$ electrode is defined by

$$\hat{I}_{a\to\text{dot}} = -\frac{\partial \hat{Q}_a}{\partial t} = \frac{i}{\hbar}[\hat{H}, \sum_k \hat{c}^\dagger_{kL} \hat{c}_{kL}],$$

which is of order $\mathcal{O}(V)$. Calculating the commutator, we have

$$\hat{I}_{\alpha\to\text{dot}} = \frac{ie}{\hbar} \sum_{k,n} V_{ka,n} \hat{c}^\dagger_{ka} \hat{d}_n - V_{ka,n} \hat{d}^\dagger_n \hat{c}_{ka}.$$

The expectation value can thus be expressed in terms of the lesser and greater Green functions we introduced in chapter II.

$$I_{a\to\text{dot}} = e \int \frac{d\omega}{2\pi\hbar} \sum_{kn} \Big[ V_{kan} G^<_{n,ka}(\omega) - V^*_{kan} G^<_{k,an}(\omega) \Big]. \tag{4.19}$$

The difficulty is to calculate these (non-equilibrium) Green functions. Fortunately, we can express them using the Keldysh techniques (that we will not cover neither describe qualitatively) in terms of simple expressions.

Considering the simple case of a symmetrical coupling of the right and left electrodes with the box, the current between the electrodes is obtained by

$$I = \frac{1}{2}(I_{L\to\text{dot}} + I_{\text{dot}\to R}) = \frac{e}{\hbar} \int d\varepsilon \text{Tr}[\Gamma \rho_{dot}][n_L(\omega) - n_R(\omega)],$$

where $\Gamma = \Gamma^L + \Gamma^R$ and

$$\Gamma^a(\varepsilon) = \pi \rho_a \sum_{nm} V_{am}(\varepsilon) V^*_{an}(\varepsilon),$$

and $\rho_a$ is the density of states in lead $a = L, R$.

### 4.6.2 Anderson model description

Let us assume that the quantum dot can be described by the Hamiltonian of the Anderson model

$$\hat{H} = \sum_{a,k} \varepsilon_k \hat{c}^\dagger_{ka} \hat{c}_{ka} + \sum_{ka} V(\hat{c}^\dagger_{ka} \hat{d} + \text{h.c.}) + U \hat{n}_{d\uparrow} \hat{n}_{d\downarrow}.$$

We remind that the Anderson model is related to the Kondo model when the charge in the impurity (here the quantum dot) is almost conserved and equal to one. This limit does not prevent (virtual) quantum charge fluctuations. Such second order processes are called elastic cotunneling processes and are depicted in Fig. 4.10. These fluctuations are responsible of the spin-flip proecesses which at the heart of the Kondo effect.

Introducing $\Gamma \simeq \pi\rho(0)V^2$, the current can be expressed as

$$I = \frac{e\Gamma}{\hbar}\int d\omega[n_L(\omega) - n_R(\omega)]\rho_{\rm dot}(\omega), \tag{4.20}$$

We have thus obtained an expression of the current only in terms of the density of states in the dot whcih is related to the retarded Green function $G_d^r(\omega)$. This formula is remarkably simple and was derived by Meir and Wingreen in 1992 [8]. In particular, we find that the **linear** conductance $G = dI/dV$ reads

$$G = \frac{dI}{dV} = \frac{e^2\Gamma}{\hbar}\int d\omega[-\partial n_F(\omega)]\rho_{\rm dot}(\omega),$$

where $n_F$ is teh Fermi Dirac distribution function. At $T \to 0$, the derivative of the Fermi-Dirac function tends towards the Dirac distrubtion. Therefore, the linear conductance $G \to 2e^2/h$ which corresponds to the maximum possible conductance. This is called the unitary limit. Physically, the screening of the artificial spin impurity (the spin of the quantum dot) by both electrodes leads to a perfectly coherent transmitting channel between the two electrodes.

In case of asymmetric coupling, we can generalize the afoermentioned calculations to find that the linear conductance at $T = 0$ reads

$$G \to \frac{2e^2}{h}\frac{4\Gamma_L\Gamma_R}{(\Gamma_L+\Gamma_R)^2} \equiv G_U.$$

At finite temperature, and finite bias $eV \ll |\varepsilon_d|, U$, one expects from the universality of the Kondo regime

$$G \approx G_U g\left(\frac{T}{T_K}, \frac{eV}{T_K}\right),$$

where $g$ is some universal scaling function. This has been checked in numerous transport experiments in quantum dots. Experimentally, these calculations predicts that when the number of electrons in the quantum doty is odd, which means in our Anderson model description $n_d \sim 1$, the conductance at $T, eV \ll T_K$ reaches a plateau of maximum conductance which is insensitive to to $V_d \propto \varepsilon_d$ as soon as $n_d \approx 1$. This has been obversed experimentally and is reproduced in Fig. 4.10.

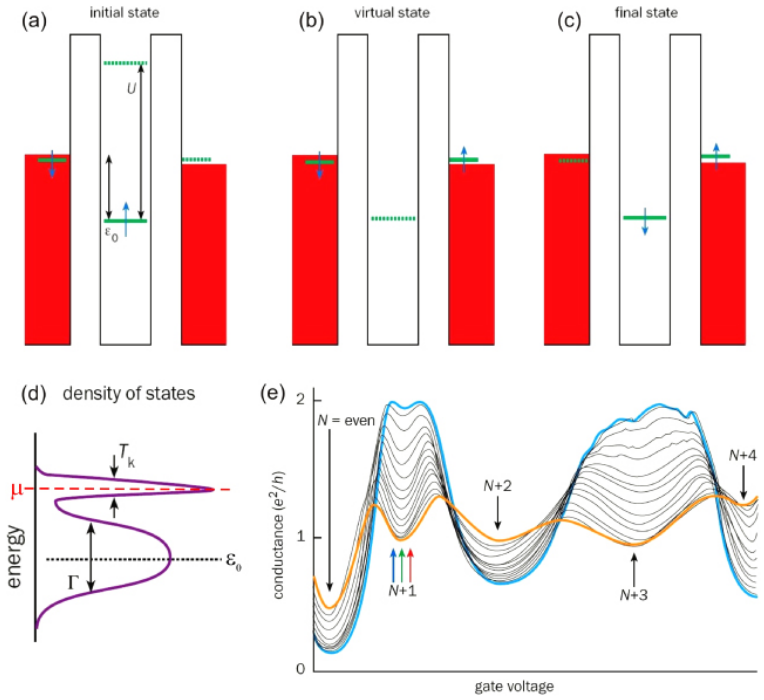


FIGURE 4.10 – Upper : cotunneling effect. Lower : Kondo resonance appearing at the Fermi level. Evolution of the conductance with temperature. At low $T \ll T_K$, plateaus of unitary conductance are observed for N=1 and N=3. From van der Wiel et al., Science 289, 2105 (2000)

# Bibliographie


[1] A. B. Bernevig and T. L. Hughes. *Topological Insulators and topological superconductors*. Oxford Uuniversity Press, 2004.

[2] P.W. Anderson. More is different, broken symmetry and the nature of the hierarchical structure of science. *Science*, 1972.

[3] A. Bruus and K. Flensberg. *Many-body quantum theory in condensed matter physics*. Princeton Uuniversity Press, 2013.

[4] J. Kondo. Resistance minimum in dilute magnetic alloys. *Progress of Theoretical Physics*, 32, 1964.

[5] P. Weiss. La variation du ferromagnï¿½tisme avec la tempï¿½rature. *Comptes rendus de l'acadï¿½mie des sciences*, 143, 1906.

[6] P. Nozieres. More is different, broken symmetry and the nature of the hierarchical structure of science. *Jour. of Low Temp. Phys.*, 17, 1942.

[7] I. K. Affleck. Conformal field theory approach to the kondo effect. *arXiv :cond-mat/9512099*, 1995.

[8] Yigal Meir and Ned S. Wingreen. Landauer formula for the current through an interacting electron region. *Phys. Rev. Lett.*, 68 :2512–2515, 1992.